Marzieh Bahador

Initial characterization of tumor heterogeneity in a syngeneic breast cancer model

International master in Molecular Medicine

Trondheim, spring 2015

Norwegian University of Science and Technology (NTNU)
Faculty of Medicine
Department of Laboratory Medicine, Children's and Woman's Health

NTNU – Trondheim
Norwegian University of
Science and Technology

HiST TRONDHEIM

CEMIR
Centre of Molecular Inflammation Research

Contents

Acknowledgements

This master project was conducted with cooperation of the faculty of medicine, department of Laboratory Medicine Children's and Women's Health (NTNU), the Centre of Molecular Inflammation Research (CEMIR) and the Faculty of Technology (HiST) in a research group led by Professor Geir Bjørkøy.

First, I want to say thank you to Professor Geir Bjørkøy who gave me the chance to work on an interesting project. I appreciate his supervision throughout this project regarding theoretical and practical issues. His guidance led me to develop an analytical and critical mindset.

Throughout this year, I have experienced the challenges of the research field, but also how fulfilling it is to overcome them. I have learnt new laboratory techniques and scientific writing. I could not have done this without receiving support from my co-supervisors Ulrike Neckmann and Jennifer Melanie Mildenberger .

I also want to say thank you to Tonje Strømmen Steigendal for helping me with the model and to Unni Nonstad and Sonja Andersen for your guidance and support. I wish to express my sincere gratitude to Marit Barstad; your respect and love for humans is inspiring.

Special thanks to Dr. Alexandre Gidon, Claire Louet, Hany Ibrahim and all CEMIR staff for their friendship and nice comments throughout my work. I take this opportunity to thank my friends Daniela Bragantini, Hele Soli, Ida Caroline Schrøder, Thea Johanne Gjerdingen, Pegah Abdollahi and Ingrid Fadum kjønstad. Thank you for being with me in tough situations and for giving me love. To Marianne Lie, Maria Sæterlid and Stine Wøien; I feel so lucky for this chance to live with you for two years. Thank you for your support and all nice moments you shared with me.

I would also like to thank my parents who thought me to be fearless, face challenges and forget tradition boundaries.

Marzieh Bahador
Trondheim, June 2015

Abstract

Breast cancer is the most common cancer in women and the main reason of cancer death in the less developed countries. Metastasis is the leading cause of death in breast cancer patients. Due to the complexity of this cascade, many aspects of metastasis are still unknown and we still lack therapy to cure or prevent metastatic breath cancer. Differences in tumor microenvironment influence tumor characteristics. Infiltrated immune cells play an important role in cancer related inflammation and may promote metastasis. Macrophages are member of innate immunity and represent a major component of infiltrated cells within solid tumors. They can be classified to classically activated macrophages (M1) and alternatively activated macrophages (M2). Tumor associated macrophages (TAMs) contribute in initiation and progression of tumors and are predominantly M2 macrophages.

Animal models have been developed for studying function of macrophages in the tumor microenvironment. However, designing *in vitro* models that may mimic interaction between cancer cells and macrophages could simplify the studies of the multiple interactions in the tumor environment and may lead to better understanding of metastatic cascade. This study was focused on a syngeneic mouse model with a functioning immune system. A model of two BALB/cfC3H mouse cell lines, 66cl4 and 67NR isolated from the same primary tumor but with a different metastatic potential was chosen. Analyzes of transcriptome sequencing data obtained from the cell lines grown in culture and as tumors in mice demonstrated numerous transcripts present in the tumor but lacking in the cell lines. These differences in the transcriptome indicated several types of stroma cells recruited into the tumors. Comparing two mouse mammary primary tumors, 66cl4 (metastatic) and 67NR (non-metastatic), suggested that almost 40% of 66cl4 and 30% of 67NR primary tumors are consist of non-tumor cells. M2 macrophages are known for their contribution in breast tumor metastasis and progression. Presence of M2 macrophages in 66cl4 primary tumor, may correlates with metastatic potential of this primary tumor. In an attempt to mimic the interaction between the two cancer cell lines and immune cells, the macrophage cell lines RAW264.7 and IC-21 cell line was tested. The obtained results suggest that these two transformed macrophage cell lines are not responsive to signal emerging from the cancer cells. This study suggests that RAW264.7 and IC-21 cell lines cannot be ideal models for studying this interaction but that primary macrophages represents a better option for studies of how cancer cells may regulate normal macrophage function.

Abbreviations

µg	Microgram (s)
µl	Microliter(s)
ARG1	Arginase1
CCL5	(C-C) motif ligand-5
CD163	Cluster differentiation 163
Ct	Threshold cycle
CXCL12	(C-X-C) motif ligand-12
DCs	Dendritic cells
DMEM	Dulbecco's modified eagle medium
ECM	Extracellular matrix
ER	Estrogen receptor
FFPE	Formalin-fixed paraffin embedded
FGF	Fibroblast growth factor
GM-CSF	granulocyte macrophage colony-stimulating factor
GM-CSF	granulocyte macrophage colony stimulating factor
H&E	Hematoxylin and Eosin
HER2	Human epidermal growth factor receptor 2
HSCs	Hematopoietic stem cells
IFN-γ	interferon(-γ)
IL4	Interleukin (4)
iNOS	Inducible nitric oxide synthase1/2
LPS	Lipopolysaccharide
LPS	Lipopolysaccharide
M	Molar
M1	classical activated macrophage
M2	alternatively activated macrophage
M-CSF	macrophage colony-stimulating factor
MDSC	Myeloid-derived suppressor cells
MHC	Major histocompatibility complex
MR	Mannose receptor
mRNA	Messenger ribonucleic acid
MS	Mannose receptor
NF-κB	Nuclear factor kappa-light-chain-enhancer of activated B cells
NK	Natural killer cell (s)
NLRs	NOD-like receptors

NO	Nitric oxide
NOS2	Nitric oxide synthase 2
PBS	Phosphate buffered saline
PCR	Polymerase chain reaction
PR	Progesterone receptor
PRRs	Pattern recognition receptor
RLRs	retinoic acid-inducible gene 1 (RIG1)-like helicase receptors
RNA	Ribonucleic acid
Rpm	Revolutions per minutes
RT-qPCR	Real—time quantitative PCR
SDF-1	stromal cell-derived factor-1
SRs	Scavenger receptors
TAMs	Tumor associated macrophages
T_C	Cytotoxic T cell
TGF-β	Transforming growth factor β
T_H1	T helper 1
TLRs	Toll like receptors
TNF	tumor necrosis factor
TNF-α	tumor necrosis factor (-α)
TREG	Regulatory T cell
VEGF	Vascular endothelial growth factor
WT	Wild type

Nomenclatures mentioned in this thesis follow the rules of HUGO Gene Nomenclature Committee for human protein (HGNC) and genes and the International Committee on Standardized Genetic Nomenclature for Mice and Mouse Genome Database (MGD) Project for mice protein and Genes.

1. Introduction

Breast cancer is the most common cancer in women. The prevalence have increased during the past years (1). Based on American Cancer Society statistics from 2013, one in eight women in the United States suffer from breast cancer during her life (2). Breast cancer is the main reason of cancer death among women in the less developed countries (3). In Norway 645 deaths was reported to the Cancer Registry of Norway in 2012 (4). Breast cancer is a heterogeneous and complex disease to study and cure (5).

1.1 Cancer Biology

Hanahan and Weinberg (6, 7) described common changes in cancer cells as "Hallmarks of cancer" that includes: Sustaining proliferative signaling, evading growth suppressors, resisting cell death, enabling replicative immortality, inducing angiogenesis, and activating invasion and metastasis. In addition to genome instability, inflammation promotes development of these hallmarks function. Moreover, reprogramming energy metabolism and evading immune destruction are emerging hallmarks (7).

Autophagy is an intracellular system for degrading damaged or extra proteins and organelles. It exists in a basal level in all cells for viability and homeostatic maintenance. In nutrient poor conditions, autophagy serves as a source of energy. Autophagy can have a paradoxical role to both suppress and promoting tumor growth in a context dependent manner. In nutrient starvation and hypoxic conditions, autophagy can be elevated in tumor cells and increase tumor survival (8).

Mutation in proto-oncogenes which is followed by their activation and loss of function of a tumor suppressor genes is obligatory in cancer development (9). Multiple biological steps are required during development of tumors. Sequential accumulation of somatic changes in preneoplastic and neoplastic cells lead to uncontrolled cellular growth, proliferation, invasion and metastasis (10). Furthermore, tumor progression depends on cellular genomic, epigenetic status (9) and also the tumor microenvironment at each stage of the tumor development. The extracellular matrix (EMC), stromal cells and infiltrating cells like immune cells constitute a complex heterogeneous tumor microenvironment. These cells secrete numerous chemokines, growth factors and matrix degrading proteins, which support tumor development(11).

1.1.1 Breast cancer classification

Due to the complexity and heterogeneity of breast cancer, there are three classifications for this disease: histopathological, biological and molecular classification. Histopathological classification is based on morphological characteristics and divides breast tumors to two main categories: invasive ductal carcinomas (IDCs) and invasive lobular carcinoma (ILC) (12). A week point of this classification is its minimal prognostic prediction (12). Biological classification is focused on prediction of responses to systematic interventions and is basically practical for clinical use. Based on this classification tumors are subdivided to highly endocrine responsive, not endocrine responsive and uncertain endocrine responsive (12). Breast cancer gene expression profiling in different studies ended up to molecular classification (13). This classification is subdivided to four groups that are variant in gene expression pastern, clinical features of treatment response and outcome. Luminal A and luminal B group highly express hormone receptors and associated genes. The HER2 group is characterized with high expression of HER2 (human epidermal growth factor receptor 2) and low expression of ER (estrogen receptor) and associated genes. Almost 15 percent of invasive breast cancers are of the basal-like group. This group is defined with high expression of basal epithelial genes and low expression of ER and HER2. Breast cancers classified in this group are mostly triple negative (ER/PR(progesterone receptor)/HER2) and are generally associated with poor prognosis (13).

1.1.2 Tumor heterogeneity

Breast cancer is a heterogeneous disease with high degree of functional, intra and intertumoral variety. These factors are critical in both tumor progression and therapeutic resistance (14). Basically, tumor heterogeneity is consist of intertumoral heterogeneity (molecular differences between patients), intratumoral heterogeneity (gain or loss of genomic alteration of tumor cells within metastatic cites), intratumoral spatial heterogeneity (somatic mutations or copy number changes within a tumor), tumor initiating ability (functional heterogeneity) and metastatic capacity (15).

1.1.3 Tumor invasion and metastasis

Metastasis is the main cause of cancer mortality and develops in the most severe forms of breast cancer (16). Novel techniques such as analysis of circulating tumor cells help to diagnose metastasis but prevention or treatment of metastatic breast cancer is still challenging (17). This

multi-step phenomenon starts with cell de-attachment from a tumor (16). In this process, cell – cell adhesion and cell adhesion to ECM are modified, allowing cells to detach (18). Free tumor cells enter blood or lymphatic vessels (intravasation) and reach distant organs. There, extravasation to the organ parenchyma, proliferation and angiogenesis leads to tumor creation and survival in a new organ (16, 17). Thus, metastatic cancer cells need to acquire abilities to survive in circulation and continue to grow in targeted organs (19). Non-tumorigenic cells may aid in the metastasis. It has been reported that platelets support tumor cells from shear stress (20) and Natural killer cell (NK) mediated cytotoxicity in blood circulation (21).

1.2 Tumor microenvironment

The tumor microenvironment contributes to make cancer a heterogeneous and complex disease. Each tumor is unique regarding molecular constitution, interaction of host and tumor cells and tumor microenvironment (22). Tumor microenvironment is composed of extracellular matrix (ECM) and normal non-mutated host cells, for instance: mesenchymal, vascular endothelial and various inflammatory cells. Cancer cells use their microenvironment as a source of nutrients, oxygen, growth factors and cytokines (23). Interaction between tumor cells and microenvironment affects primary cancer growth, invasion and metastasis (21). The tumor microenvironment is influenced by both endogenous factors (such as genomic variation and hormonal environment) and exogenous factors (dietary, environmental exposure and lifestyle) (22).

1.2.1 Extracellular matrix

ECM acts as a physical scaffold that facilitates cells adhesion, movement and cell-cell interaction. It consists of many components including glycoproteins like laminin, fibronectin, elastin and fluid produced by cells. All these elements can influence tumor cells in different ways (19). Stromal cells like fibroblasts, endothelial cells, adipocytes and different immune cells are embedded in ECM (21, 24). It is noteworthy that stromal cells of tumor microenvironment are heterogeneous both in their proportion and activation status. These cells play diverse functions in different stages of tumor development (21). For example: adipocytes which are the most frequent adjacent cells around breast cancer cells (25), provide fatty acids which contribute in tumor growth (26). Activated endothelial cells facilitate angiogenesis in both primary and metastatic tumor (27) and they can also contribute initiating breast cancer (25). Fibroblasts in ECM exist in high number and enhance metastasis in premalignant and malignant breast epithelial cells (21). Moreover, fibroblasts in the breast tumor microenvironment may induce therapeutic resistance. It is notable, stromal cells in the breast tumor environment can also modify phenotype of the tumor cells (25). For instance, IL6 secreted from cancer associated fibroblasts induced invasive phenotype in breast cancer (28).

1.2.2 Immune cells

A complex composition of immune and inflammatory cells exists in tumor microenvironment (23). Different bone marrow-derived cells can be seen in the stroma of tumors, including

myeloid and lymphoid lineage cells. Typical myeloid cells found in tumors are macrophages, neutrophils and myeloid-derived suppressor cells (MDSC) (Figure 1.1) (19). Lymphoid lineage cells are also present in tumor microenvironment and demonstrate distinct functions depending on their types. For instance, CD8+ cytotoxic T lymphocytes (T_c) induce apoptosis in cancer cells by releasing perforin and granzyme (21). T helper type 1 (T_H1) cells support T_c cells in tumor rejection, while T helper 2 (T_H2) cells and regulatory T (T_{REG}) cells cooperate in suppressing activation of T_c cells (29). Furthermore, B lymphocytes secrete pro-tumorigenic cytokines and alter T_H1 and T_H2 ratios (21).

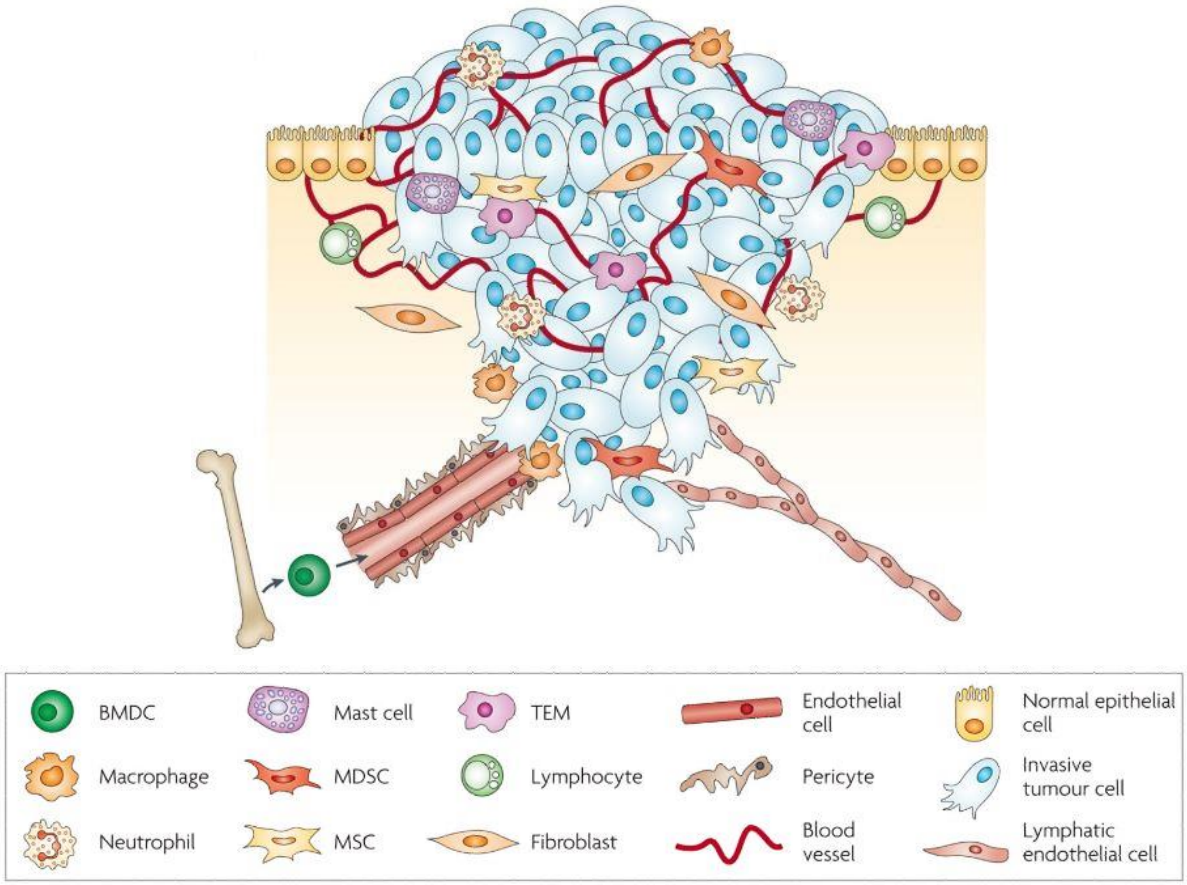

Figure 1.1: Schematic illustration of the primary cells in the tumor microenvironment

Tumor microenvironment consists of endothelial cells from blood and lymph, fibroblast and different bone marrow-derived cells for example; macrophages, myeloid derived suppressor cells (MDSC), TIE2-expressing monocytes (TEMs), mast cells and mesenchymal stem cells (MSCs).These cells are recruited by cancer cells and have different functions. The figure is adopted from Joyce, J. A. *et al.,* 2009 (19).

Cancer cells able to form tumors are successful in escaping from immune system and also in modifying immune cell types in favor of tumor cells (24). Bone marrow-derived cells, myeloid lineage in particular, are recruited to primary and metastatic tumors. They can have opposing functions in promoting or inhibiting tumor growth. Chemokines and growth factors such as

chemokine (C-C motif) ligand 5 (CCL5)/RANTES and CXCL12/SDF-1 produced by stromal and tumor cells recruit monocytes which differentiate to macrophages in the tumor site (30). Existence of macrophages in the tumor tissue correlate with poor prognostic, higher tumor grade and increased mortality rate (31).

MDSCs are heterogeneous early myeloid cells that can be generated in response to cancer derived factors and cause immune response suppression. These cells produce arginase1 (ARG1), inducible nitric oxide synthase (NOS2) also known as iNOS and reactive oxygen species that create an immune environment which contributes in tumor progression (32). MDSCs activation can also protect metastatic cancer cells from T_c cells and NK cells (24, 32). Identification of mechanisms and molecular events within breast cancer microenvironment that contribute to tumor progression can indicate new therapeutic targets (25). Different cell types can be investigated by using cell specific markers. cell markers can be investigated (23). Table I shows some markers of immune cells present in breast tumor microenvironment and that can be analyzed for experimental purposes (see appendix).

1.2.3 Cancer-related inflammation and infiltrated immune cells

In 1867, Virchow *et al*., described the role of inflammation in cancer development (33). Recent evidence supports the role of inflammation in breast cancer regulation (34). Harold and Dvorak, 1986 first described tumors as "wounds that do not heal" (35).Studies have shown that inflammation that resulted from tissue injury, promotes cellular proliferation and neoplastic transformation (36). Infiltrated immune cells are important players in cancer related inflammation (33). Elimination of mature B lymphocytes and subsequent decrease in innate immune cells recruitment in a transgenic mouse model demonstrates the role of chronic inflammation in promotion of *de novo* carcinogenesis (37). A wide number of chemokines recruit leukocytes to the inflammatory site (33). Macrophages constitute the major inflammatory cell type in the stroma of different tumors (38). Increased number and activity of macrophages and other MDSC in chronic inflammation is possibly due to the B cells and T helper17 (T_H17) cells activation (29). These characteristics make it eligible to study the function of macrophages as an inflammatory cell that promote cancer progression.

1.3 Macrophages

Circulating monocytes differentiate into macrophage and dendritic cells in body tissues in the steady state and in response to inflammation (39, 40). Monocyte-macrophages lineage are well known for their diversity and plasticity (30). In the tissues, macrophages can be activated by both endogenous and exogenous factors (41).

Macrophages play a critical role in innate immunity. They are phagocytic cells are recognize their target through receptors of the cell membrane (42). A multitude of receptors are expressed on the surface of macrophages (39). For instance, scavenger receptors (SRs), such as CD163 (43), bind to modified lipoproteins (44) on the surface of apoptotic and necrotic cells. These receptors opsonize pathogens and cell debris and initiate phagocytosis. Subsequently, macrophages engulf opsonized pathogens and debris into a phagosome and digest the components. Signaling pattern recognition receptors (PRRs) including toll-like receptors (TLRs), NOD-like receptors (NLRs) and retinoic acid-inducible gene 1 (RIG1)-like helicase receptors (RLRs) are also expressed on the surface of macrophages. TLRs are able to recognize non-self (PAMS) and damaged cells (DAMS) in the cytoplasm or on the cell surface of the cells and trigger downstream signaling mechanisms that activates transcriptional mechanisms. This process will finally result in clearance of the insult and release of different cytokines and chemokines in order to respond to their environment (39). Macrophages can also be activated in response to cytokines such as IFN-γ. Anti-inflammatory molecules such as IL4 and IL13 can also activate macrophages (45). It is explained in more detail in figure 1.2 and rest of section 1.3 of the introduction chapter.

Macrophages are the most common infiltrated cells in the microenvironment of many tumors (46). High number of macrophages in breast tumor stroma correlates with tumor size and reduced breast cancer survival (47).

Macrophages can be classified based on their function. There exists a spectrum of subtypes from classically activated macrophages (type I macrophage, M1) (45) to alternatively activated macrophages (type II macrophages, M2) as the most extreme samples (Figure 1.2) (45, 48). These heterogeneous cells can change their polarization and function in response to different environmental signals (49) such as microbial antigen and T_H1 or T_H2 derived cytokines (45, 50) and also tumor products (51). The remarkable contribution of macrophages in breast tumor progression is the main focus for the current study.

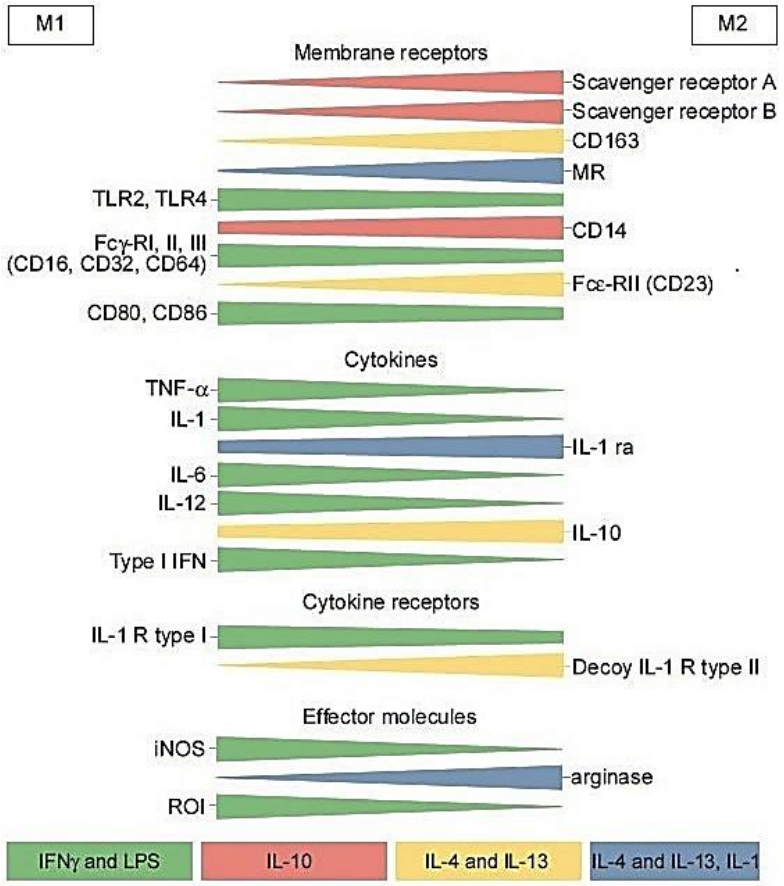

Figure 1.2: Macrophages, spectrum of subtypes
In this figure, molecules that are induced by IFN-γ and LPS (classical activation) are displayed in green (for M1) and they express opsonic receptors (such as Fcγ-RI/CD64 and Fcγ-RI/CD32). For M2 macrophages, molecules induced by IL4 and IL13 displayed in yellow, IL10 in red and IL4, IL13 and IL1 displayed in blue. M2 macrophages poses high number of mannose receptor (MS) (modified) (45).

1.3.1 Macrophage phenotypes

The alternative activation of macrophages was first described in 1992 Stein M *et al*.,(48). An *in vitro* model evidenced that interleukin 4 (IL4) induces a polarization, distinct from macrophages induced by interferon γ (IFN-γ). In this model stimulation of peritoneal macrophages with IL4, enhance MR expression and activity compared to macrophages stimulated with IFN-γ. Macrophage can be schematically divided to M1 (pro-inflammatory) and M2 (anti-inflammatory) (41, 52). Macrophage activation status should be studied as a continuum ranging from pro-inflammatory (M1) to anti-inflammatory (M2) rather than discrete phenotypes (53).

Classically activated macrophages respond to pathogens and are important players of the innate immune defense (54). Monocytes differentiate to M1 in the presence of exogenous pathogens associated molecules like the bacterial Lipopolysaccharide (LPS) (55, 56), endogenous danger signals such as heat shock proteins (41) or endogenous cytokines such as IFN-γ (57), tumor

necrosis factor (TNF) and granulocyte macrophage colony stimulating factor (GM-CSF) (41, 56). M1 activated cells can be distinguished by elongated appearance (41). Moreover, M1 macrophages secrete pro-inflammatory cytokines such as IL23 and IL12 (56). These factors, together with phagocytosis, are important for the removal of pathogens and danger signals and initiation of an immune response in the early phases of wounds' healing (58). M1 macrophages have anti-tumor activity (59). IL12 secreted from M1 macrophages can suppress metastasis (60) and stimulates T cell (61) and NK cell cytotoxicity against tumor cells (62). Nitric oxide (NO) produced by macrophages is cytotoxic and plays role in suppression of tumor growth (63) and metastasis (64). Binding of LPS to TLR4 on the surface of M1 macrophage leads to NO production by NOS2 through NF-κB activation (65).

On the other hand, M2 macrophages exhibit anti-inflammatory functions and regulate wound healing (39). Monocytes differentiate to M2 in the presence of TH2 cytokines such as interleukin 4 (IL4), IL10, IL13 (57, 66) and macrophage colony stimulating factor (M-CSF) (41, 56). IL4 and IL13 cytokines elevate expression of MR by M2 macrophages and stimulates *in vitro* activity of arginase, whereas elevated activity of NOS2 by IFN-γ stimulation inhibits arginase activity. Arginase is an intracellular enzyme (66) that regulates wound healing and fibrosis. This enzyme inhibits antitumor T_C cell response and converts L-Arginine to urea and L-ornithine that are main substrates for polyamines production. Polyamines are necessary for cell cycle progression (67).

In vitro stimulated M2 macrophage induces spheroid phenotype (41). Generally, M2 macrophages promote angiogenesis and contribute in the tissue remodeling and repair by release of vascular endothelial growth factor (VEGF), transforming growth factor β (TGF-β) or fibroblast growth factor (FGF) in wounds (58). In the tumor micro environment, M2 macrophages show the same functions in favor of tumor progression (52). This paradoxical role of macrophages has not been completely understood (56). A summary of M1 and M2 macrophage cytokine, their activation and function can be seen in figure 1.3 (68).

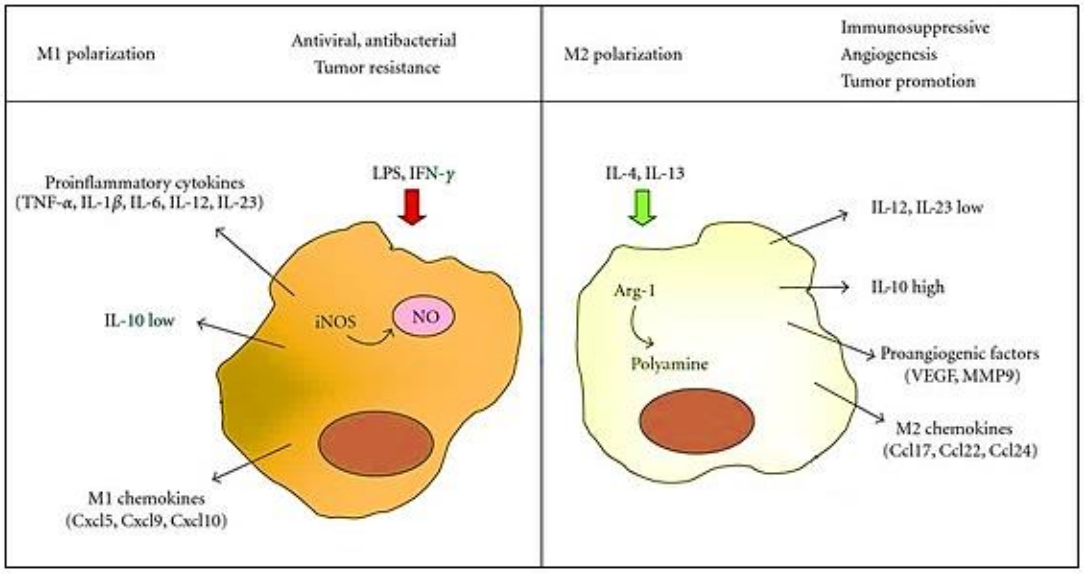

Figure 1.3: Schematic M1 and M2 macrophages function and activation
M1 and M2 macrophages modify their function in response to the environmental stimuli. M1 macrophages are induced by LPS and IFN-γ and release different proinflammatory cytokines such as IL6 and IL1β. M1 polarized macrophage demonstrate antiviral, antimicrobial and tumor resistance function .In contrary, M2 macrophages can be induced by IL4 and IL13 and release different chemokines and proangiogenic factors. M2 macrophages can contribute in immunosuppression, angiogenesis and tumor promotion (modified) (68).

1.3.2 Tumor-associated macrophages

Macrophage phenotypes change during the malignancy process. Initially, M1 macrophages induce inflammation around epithelial lesions by secreting TNFα and IL12 (69). Secretion of variety of growth factors from M1 macrophages results in high proliferation of epithelial cells to replace damaged cells (70). This high proliferation rate can lead to acquisition of mutations in the epithelial cells. Because of hyperplastic lesion progression, intraepithelial neoplasia will be formed. Chemo attractants and a variety of chemokines such as CCL-2 recruit monocytes to the site of inflammation from blood circulation (71). Recruited monocytes differentiate to tumor-associated macrophages (TAM) in the presence of M-CSF released by neoplastic cells (72). These macrophages mostly resemble M2 like phenotype (71, 73) and function (74, 75). In addition, mouse mammary tumor gene profiling data demonstrated that TAMs are predominantly M2 macrophages.

TAMs have the leading role in cancer-related inflammation. As reviewed by M. Liguori *et al*., TAMs constantly contribute in deposition and degradation of the ECM which results in release of matrix-bound growth factors (72). ECM remodeling and basement membrane fragmentation, promote tumor cell motility and invasion (76). Down-regulation of adaptive immune system by TAMs goes along with production of cytokines such as IL10 and TGFβ. Produced cytokines recruit and stimulate T_{REG} and recruit T_H2 lymphocytes that inhibits T_H1 activation and induce

naive T lymphocytes. TAMs also contribute to angiogenesis by producing proangiogenic cytokines (52) such as VEGF and FGF. Some of the cytokines, chemokines and proteases associated with tumor angiogenesis, metastasis and immune suppression are summarized in figure1.4 (73). However, the function of TAMs in initiation and progression of tumors has not been completely understood (77).

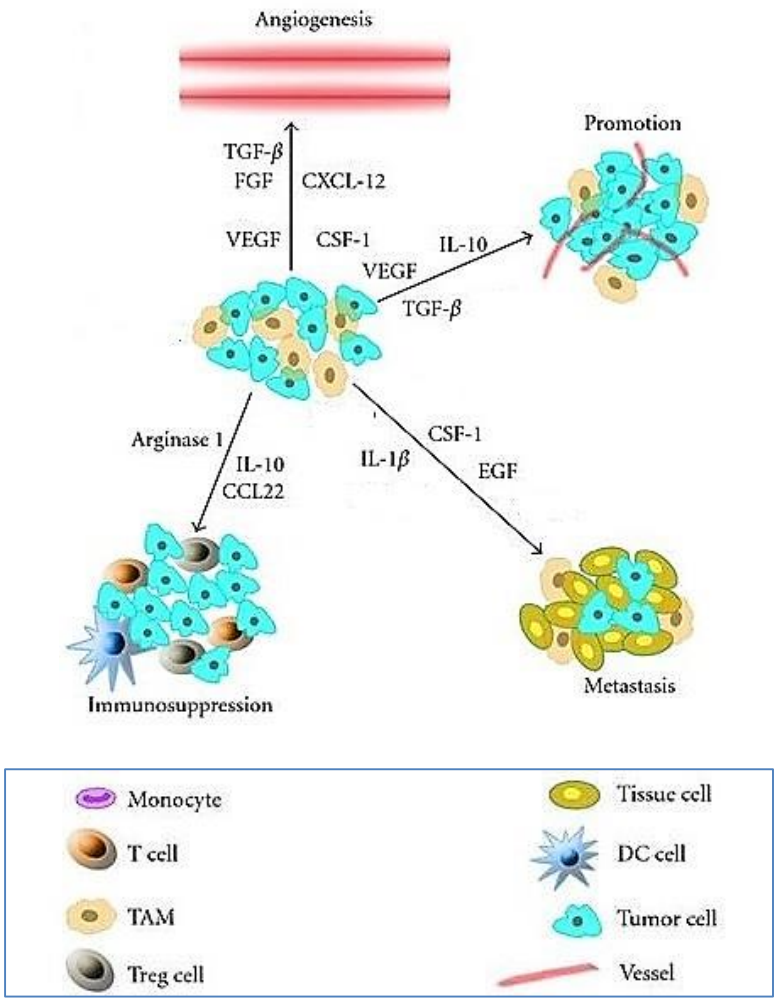

Figure 1.4: TAM function in tumor progression
TAM contributes in tumor progression. M2 macrophages are predominant in tumor microenvironment. They express cytokines, chemokines and proteases that increase tumor metastasis, angiogenesis and immune suppression (modified) (73).

1.3.3 Macrophages and tumor energy acquirement

Tumors growth beyond 1-2 mm in diameter acquires induction of new blood vessels for proliferation and metastasis (78-80). Angiogenesis is a process in which capillaries sprout from endothelium of the existing vascular networks (79, 81). This process facilitate supply of oxygen and nutrients, evacuate metabolic waste and contributes in metastasis (7, 82). It is now well

established that breast cancer, as many other types of cancer, is dependent on angiogenesis that correlates with invasiveness and poor survival (83, 84). Components of the tumor microenvironment are of extreme importance in angiogenesis (85). TAMs influence angiogenesis by expression of angiogenic factors such as VEGF (33) and platelet-derived endothelial cell growth factors and also TNF-α and IL8 in hypoxic conditions (86). Moreover, pericytes that are located on the surface of capillaries contribute in stabilizing vessel wall, controlling endothelial cell proliferation and new capillaries growth (87).

Autophagy is an intracellular degradation system in which breaking down cellular organelles results in re-using sources of energy in the cell. This catabolism will be used for biosynthesis and energy metabolism. Autophagy is critical during fasting but also removes damaged organelles, misfolded proteins and microorganisms from the cytoplasm. It is present in a basal level in cells but can also be upregulated in cellular stress such as nutrient deficiency representing a survival mechanism in situations of cellular stress (88, 89). Martinez-Outschoorn and his colleagues' experimental model explains that epithelial cancer cells induce autophagy in the tumor stroma by oxidative stress and initiate energy transfer from tumor stroma which enhances tumor growth (90). They have called this model "Battery-Operated Tumor Growth" (91).

Furthermore, autophagy is important in maintenance and differentiation of hematopoietic stem cells (HSCs), differentiation of monocytes into macrophages and also macrophage recruitment (92).

1.3.4 Macrophages in Breast cancer

Plethora of macrophages can be detected in the nipple aspirate of women from reproductive age. An experimental model demonstrated that high number of macrophages is recruited to the developing terminal end bud (TEB) of the mammary gland of mice. They are abundant in the base and shaft of the TEB and can also be found in TEB itself. Notably, collagen fiber network facilitate macrophage movement (Figure1.5). Macrophages that are present in mammary gland are associated with immune suppression and tumor progression (93). This also correlate with poor prognosis(94), increased vascular density(95), tumor size and mortality (47).

It is now well established that TAMs play a prominent function in breast carcinogenesis (96-98). They can make up almost half of the breast tumor cell mass (99) which correlates with poor prognosis (98, 100). Breast tumors present a hypoxic condition such as many other solid tumors (101). This condition enhances macrophage recruitment to the breast tumor

environment (102). Recruited macrophages are entrapped in the hypoxic area (103). As Leek RD and his colleagues has shown, accumulation of TAMs correlates with angiogenesis in breast tumor (104).

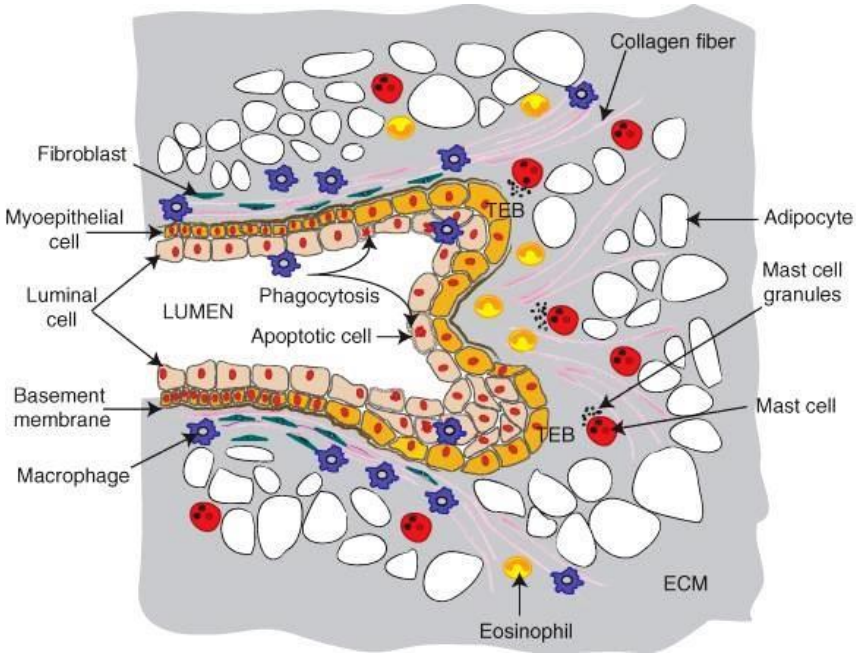

Figure1.5: Topology on macrophages in TEB
In mice, TEB is surrounded by fibroblastic stroma and adipocytes. Numerous numbers of immune cells such as macrophages are found in TEB. Preferred areas of different cells are indicated (93).

1.3.5 Role of macrophages in breast tumor metastasis

Breast tumor can metastasize to lung, bone, liver, lymph nodes (19) and pleura (105). TAMs enhance breast cancer metastasis by secreting a wide range of cytokines and chemokines (106). CCL18 is mostly produced by M2 macrophages, which are the most abundant macrophages in breast tumor. CCL18 production in breast tumor correlates with invasion, metastasis and reduced patient survival (98). CCL2 is another chemokine which is over expressed in breast cancer and associated with high metastatic rate and subsequent increased mortality in mice. L.Bonapace and her colleagues demonstrated that treatment by anti-CCL2 reduced macrophages in a primary tumor of 4T1.2 cells, derived from BALB/cfC3H mouse (107). Moreover, CXCL12 receptor (CXCR4) is expressed on macrophages and tumor cells. Tumor cell motility and invasion can be stimulated by production of CXCL12 in the mouse model (71). In addition, expression of angiogenesis factors such as VEGF by TAMs, promotes vasculogenesis in the breast tumor, which is vital for tumor metastasis (108). This aspect is

explained in detail in section 1.3.2. In addition, macrophages help tumor cell egression and intravasation by clustering on the blood vessel (71).

Present treatment options are not effective to cure metastatic breast cancer (109). Hopefully, a better comprehension of the metastatic cascade can lead to new therapeutic methods (110).

1.4 Model systems of cancer development

Varity of experimental models can be used in order to study different aspects of the cancer. Transgenic mouse models have been used for studying role of a distinct genes in breast carcinogenesis (111). For studying effect of different cytokines and growth factors, human cancer cell can be studied in cell culture. Cytokines and growth factors can be added to the culture and then tumor cell response can be studied. In addition, cancer cells can be co-cultured with stromal cells such as fibroblasts. However, results from such models are difficult to interpret and components of tumor microenvironment such as immune cells are absent. Using human cancer cell lines and implanting the cells in the mouse is another option. In such models tumor cells and microenvironment are from different origin, immune cells are missing. Therefore, this model is not optimal for studying tumor heterogeneity. Using human patient tumor and implanting tumor in an immunodeficient mouse can include original tumor heterogeneity and micro environmental compartments such as fibroblast to the model, but immune cells are absent in this model as well. In syngeneic spontaneous models, mouse tumor cell lines are used, host immune cells are present and microenvironment is intact (112). Immune system of mouse is normal and is from the same species with tumor cells. This feature represent the real life situation that is important in the studies that are focused on interaction between tumor and host microenvironment. However, this model may not represent genetic and clinical complexity of human tumors (113). Autochthonous murine tumor models are spontaneous or chemical, viral and physical induced tumors that include many tumor micro environmental features. This model closely mimic human tumors than transplant tumor models but more expensive and with lower throughput. Other disadvantages of this model are stochastic variability and lack of spontaneous metastasis (114, 115).

1.4.1 The 4T1 syngeneic BALB/cfC3H mouse breast Cancer Model

Our laboratory has access to five mouse breast cancer cell lines (67NR, 168FARN, 4TO7, 66cl4 and 4T1). These cell lines originate from a spontaneous arising BALB/cfC3H mouse mammary tumor (116, 117). Their different metastatic ability have been documented in many studies (Table1.1) (118, 119). This basal-like model (120) gives a valuable opportunity to study interaction of primary tumors and immune cells in a heterogeneous microenvironment by designing a syngeneic, non-manipulated mouse model with a functioning immune system.

Earlier studies by the Bjørkøy group have investigated the autophagic flux of these five breast cancer cell lines. Unpublished recent *in vitro* experiments demonstrated that 66cl4 cell line has

higher expression of autophagic markers such as p62 and LC3B-II and higher autophagy flux compared to 67NR cell line. No significant expression of autophagic markers in other cell lines was observed. Therefore, 66cl4 and 67NR were chosen for further analysis. It was hypnotized that the increased autophagy flux of 66cl4 lead to better availability of nutrients under starving conditions and thus more aggressive growth and metastasis. As previously mentioned, tumors are comprised of different cell types that may contribute to different aspects of carcinogenesis. Accordingly, autophagy could be differently regulated in different cell types of the tumor microenvironment. Most importantly, the tumors of both cell lines have been RNA sequenced, which can represent valuable information regarding gene expression, but also this data does not take into account the contribution of different cell types in the tumor. Therefore, it makes an obligation of characterizing different cell types in the primary tumor and their composition to allow a more precise interpretation of further results.

Table1.1. Metastatic properties of 5 cell lines isolated from a spontaneous arising mammary tumor BALB/cfC3H (118, 119)

Cell line	**67NR**	**168FARN**	**4TO7**	**66cl4**	**4T1**
Primary tumor	Yes	Yes	Yes	Yes	Yes
Metastatic potential	No	Yes	Yes	Yes	Yes
		Micro metastases to lymph nodes	Micro metastases to the lung, lymph nodes, blood	Lungs	lungs, bones, lymph nodes, blood, liver, brain, stomach etc
	-	+	+(+)	+++	++++

1.5 Aim of the study

The tumor microenvironment plays a prominent function in carcinogenesis and TAMs are an important component of the tumor stroma (96, 97). A better understanding of district functions of mammalian immune system in both suppression and progression of breast tumors can help to define the interplay between immune cells and breast cancer progression.

The aim of the present study was to investigate BALB/cfC3H mouse spontaneous breast tumor model heterogeneity. The first important step was to estimate the number of normal, non-transformed cells present in primary tumors of 66cl4 and 67NR cells. Secondary, it was of interest to determine if macrophages were present in the tumor and try to define their phenotype. If signs of differences in macrophage phenotype could be found, attempts to design an *in vitro* model to study the interaction between the macrophage and cancer cell lines should be initiated.

2. Material and methods

2.1 Equipment

Microtome Leica RM2235	Leica Microsystems, Germany
Confocal microscope LSM 510 Meta	Zeiss, Germany
EVOS® FL Auto Cell Imaging System	Life technologies, USA
Zeiss Primo Vert Inverted Microscope	Zeiss, Germany
Odyssey CLx 9140 scanner	LI-COR, USA
Z1 COULTER COUNTER	Beckman coulter, USA
Spectronic GENESYS 20 Visible Spectrophotometer 4004-2	Thermo electron cooperation, USA
NanoDrop 1000 Spectrophotometer	Thermo Fisher Scientific, USA
Thermal cycler C1000	Bio-Rad Laboratories, USA
Thermal cycler 2720	Applied Biosystems, Thermo Fisher Scientific, USA
StepOnePlus Real-Time PCR system, version 2.0.46	Applied Biosystems, Thermo Fisher scientific, USA

2.2 Consumables

Chamber Coverglass (#155411)	Nunc, Thermo Fisher, USA
Dako pen (#S200230)	Dako, Denmark A/S
Immobilon-p PVDF Transfer Membrane (#IPVH304Fo)	Millipore, USA
MS MACS separation columns (#130-042-201)	Miltenyi Biotec, Germany
NuPAGE® Novex® 10% Bis-Tris Protein Gels, 1.0 mm, 10 well (#NP0301BOX)	Life technologies, USA
NuPAGE® Novex® 12% Bis-Tris Protein Gels, 1.0 mm, 12 well (#NP0342BOX)	Life technologies, USA
NuPAGE® Novex® 4-12% Bis-Tris Protein Gels, 1.0 mm, 12 well (#NP0321BOX)	Life technologies, USA

Superfrost Plus microscope slide (#4951PLUS4)	Thermo Fisher Scientific, USA

2.3 Buffers, media and solutions

20xMOPS SDS running buffer (#NP0001-02)	Life Technologies, USA
Bio-Rad Protein Assay Dye Reagent Concentrate (#500-0006)	Bio-Rad Laboratories, USA
Blood and cell culture DNA mini kit (#13323)	Qiagen, Netherland
cOmplete, EDTA-free (#11873580001)	Roche, Switzerland
Dako Target Retrieval Solution (#S169984-2)	Dako, Denmark A/S
Dimethyl sulfoxide (DMSO) (#D2650)	SIGMA-ALDRICH, USA
DL-Dithiothreitol (DTT) (#45-43816-50ML)	SIGMA-ALDRICH, USA
DRAQ5 (#4084)	Cell Signaling technology, USA
Dulbecco's Modified Eagle's medium(DMEM) (#D5796)	SIGMA-ALDRICH, USA
Dulbecco's phosphate buffered saline (DPBS) (#D8537)	SIGMA-ALDRICH, USA
Fetal bovine/calf serum (FBS)/(FCS) (#1027)	Gibco, Life technologies , USA
Gentamicin (#157100-049)	Gibco, Life technologies , USA
ISOTON II (#854619)	Beckman coulter, USA
L-Glutamine (#17-605E)	Lonza, Switzerland
LPS-EB Ultrapure (#tlrl-3pelps)	Invitrogen, USA
Non-essential-amino acid solution 100x (#M7145)	SIGMA-ALDRICH, USA
NuPAGE® LDS Sample Buffer (#NP0007)	Thermo Fisher Scientific, USA
NuPAGE® Transfer Buffer (#NP0006-1)	Life Technologies, USA
Odyssey two-color protein molecular weight marker(IR dye 400) (# 928-40000)	LI-COR Biosciences, USA

Odyssey® Blocking Buffer, TBS (# 927-50000)	LI-COR Biosciences, USA
Paraformaldehyde 16% (PFA) (#43368)	Alfa Aesar, USA
Penicillin-Streptomycin (#P0781)	SIGMA-ALDRICH, USA
Phosphatase inhibitors cocktail 2 (#P5726)	SIGMA-ALDRICH, USA
Phosphatase inhibitors cocktail 3 (#P0044)	SIGMA-ALDRICH, USA
QuantiTect Reverse Transcription Kit (#205311)	Qiagen, Netherland
QuantiTect SYBR green PCR kit (#204141)	Qiagen, Netherland
Recombinant Murine IFN-γ (#315-05)	Peprotech, USA
Recombinant Murine IL4 (#214-14)	Peprotech, USA
RNA protect cell reagent (#76526)	Qiagen, Netherland
RNAprotect Cell Reagent (#74624)	Qiagen, Netherland
RNeasy Micro kit (#74004)	Qiagen, Netherland
RPMI-1640 Medium (#R8758)	SIGMA-ALDRICH, USA
TaqMan genotyping master mix (#4371355)	Life technologies, USA
Triton x-100 (#T8787)	SIGMA-ALDRICH, USA
Trypsin-Versene (EDTA) mixture (1X) (#BE17-161E)	Lonza, Switzerland
Urea (#U5378)	SIGMA-ALDRICH, USA
Vectashield, mounting medium with Dapi (#H-150)	Vector Laboratories, UK

2.4 Computer programs

GraphPad	
Image Studio	LI-COR Inc., U.S.A
ND-1000 version 3.2.1	Thermo Fisher Scientific, USA
Step one versions 2.2 and 2.3	Life Technologies, USA
ZEN versions Blue and Gray	Zeiss, Germany

2.5 Cell lines

66cl4	Barbara Ann Karmanos Cancer Institute

67NR	Barbara Ann Karmanos Cancer Institute
IC-21	
Raw 264.7	

2.6 Primary tumors

This project was focused on analyzing 66cl4 and 67NR primary tumors. 66cl4 and 67NR mouse breast tumor cells (500,000 cells per animal) have been injected in to the fat pad of BALB/cfC3H mouse. After 3-4 weeks tumors were 1-1, 5 cm and large enough to be removed from the mouse. Primary tumors that resulted from this stage have been used for mRNA sequencing in Bjørkøy group and protein and DNA isolations in this master study.

This procedure has been done two times. For the second round, 66cl4 and 67NR cell lines that have injected to the mouse had been infected with Mission TRC2 Control Transduction Particle puro TurboFFP shRNA (Sigma #SHC204V) to stably express GFP in the tumors. Obtained tumors have been used for tumor section preparation. For this purpose tumor samples were fixated in 4^{o}C formalin for 1 day and then they have been stored in 70% ETOH /PBS and paraffin embedding.

2.7 Cell culture

67NR and 66cl4

67NR and 66cl4 are adherent BALB/cfC3H mouse cell lines established from a primary breast tumor. These cells were cultured according to the guideline that is provided by Barbara Ann Karmanos Cancer Institute. Dulbecco's Modified Eagle's medium (DMEM) has been suggested by aforesaid institute for maintenance of these cell lines. Based on the Karmanos Cancer Institute guideline, medium was supplemented with 10% fetal bovine serum (FBS), 1% L-glutamine, 1% Non-essential amino acid solution and 1% Penicillin/streptomycin.

RAW 264.7

RAW 264.7 cells are mouse-derived macrophages that have been established from a tumor induced by Abelson murine leukemia virus (ATCC® TIB-71™). This adherent cell line was cultured in RPMI-1640 medium supplemented with 10% fetal bovine serum (FBS), 1% L-glutamine, 1% Non-essential amino acid solution and 1% Penicillin/streptomycin.

IC21

IC-21 is an adherent cell line that was established by transformation of normal C57BL/6mouse peritoneal macrophages with SV40 virus. It demonstrates many characteristics of normal mouse macrophages such as phagocytic and cytolytic properties. This cell line has been provided in cooperation with CEMIR and was cultured based on ATCC guidelines (ATCC® TIB-186™) in RPMI-1640 medium. This medium was supplemented with 10% fetal calf serum (FCS), 0,034 % L-Glutamine and 1% gentamicin. Medium of these adherent cells should be changed 3 times a week due to the high acid production.

2.7.1 Taking up the cells

Cells have been kept in a cryotube in 20% FBS and 10% DMSO in the liquid nitrogen storage container. They were thawed in 37ºC water bath. Cells were taken up in 5-10 ml medium and were transferred to a 15 ml tube. After centrifuging in 1500 rpm for 5 minutes, 5ml cell line specific medium was added to the cells. Dissolved cell pellet was transferred to a 25cm^2 culture flask with 5ml medium and placed in a 5%CO2 humidified incubator at 37ºC. Medium was changed after the cells had attached. Cells were routinely kept in the incubator, which provides optimized condition for cell growth.

2.7.2 Subcultivation of cells

Subcultivation was after cells reached 70-80% confluency by removing the old medium, washing the cells twice with phosphate buffered saline (PBS). For detaching 66cl4 and 67NR cell lines, trypsin added and for RAW264.7 and IC21 cells PBS plus 0,02% EDTA was added. It was followed by addition of specific medium for each cell line. Suitable number of cells was added to a new culture flask filled by adequate medium. For running a new experiment, cells were ready after subcultivateed for three times. The cell line which was subcultivated for more than 20 passages was discarded.

2.7.3 Conditioned medium preparation

Conditioned medium of 66cl4 and 67NR cells was prepared from two different cell passage numbers. Cells were counted by adding cell suspension (20µl) to isoton II diluent (10ml) (Beckmann coulter) using Z1 Beckman cell and particle counter (Beckmann coulter). Adequate number of cells (200.000) were seeded in 6cm dishes (9.5cm^2). Cells were left in an incubator for 48 hours. Medium of the plate was collected and centrifuged at 1500g for 10 minutes. Supernatant was aliquoted to 1.5 ml eppendorf tubes.

2.7.4 Preserving Cells in Liquid Nitrogen

Cells were washed with PBS and detached using PBS-0.02% EDTA or trypsin. Medium was added to detached cells then cells were suspended and counted. Three millions of 66cl4, two millions of 67NR and RAW264.7 cells were centrifuged in 1500rpm for 5 minutes. Cell pellet was resuspended in the freezing medium containing 20%FBS and 10%DMSO. Cryotubes containing 500µl of the cell suspension were incubated in styropore box at -80^oC for 48 hours before transferring to the liquid nitrogen tank.

2.8 Confocal microscopy

Confocal laser scanning microscopy (CLSM) is based on molecule excitement and subsequent emitted florescent. CLSM is consist of a laser light with a defined wavelength which produce a beam of light that directed to the specimen and can be detected and converted to a electrical signal that creates a photo. As it is illustrated in figure 2.1 pin hole that was embedded in this microscope allows only beams from the focal plane to reach the detector which leads to production of images with great resolution (121).

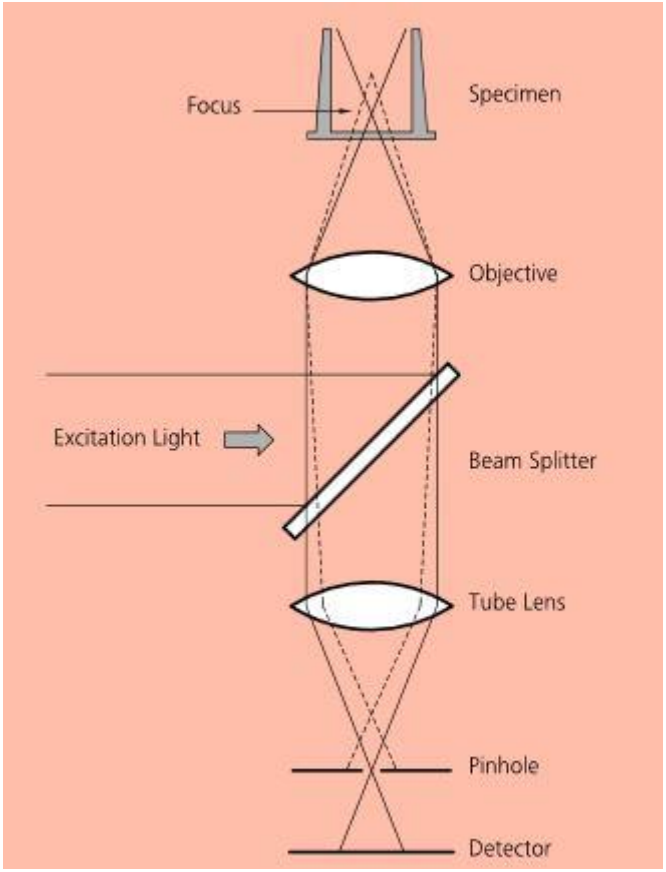

Figure 2.1: Pinholes function in confocal microscope. Small pinhole designed in confocal microscope allows only beams from the focal plane to reach the detector. Therefore, absence of stray light gives a clear image (121).

2.8.1 Seeding and fixating cells

Cells were counted and appropriate amount of cells were seeded in in a Chambered cover glass. Afterwards cells were treated by desired concentration of conditioned medium of 66cl4 and 67NR (section2.7.2) or ligands (LPS) and cytokines (IFN-γ, IL4) after cells attachment to the surface at relevant time points. Cells were fixated adding 4% paraformaldehyde (PFA) to the medium and left on shaker for 10 minutes at room temperature. Fixated cells were washed once with PBS.

2.8.2 Immunostaining

Before staining cells should be permeabilized, therefore 400µl ice-cold methanol was added to the wells. Chambered cover glasses were incubated on ice for 10 minutes and washed once with PBS. Permeabilization was followed by blocking in order to reduce non-specific binding. Therefore, PBS with 3 % goat serum (200µl/well) was added because goat secondary antibodies was used. Cells were incubated in blocking buffer at 4^{o}C on shaker, overnight.

Both primary and secondary antibodies were diluted in PBS with 1 % goat serum. Primary antibodies (150µl/well) were added and incubated on shaker at 4^{o}C overnight or room temperature for1 hour (Table2.1). Negative controls contained no primary antibody. Cells were washed 6x5 minutes on shaker using PBS (200 µl) and incubated 60 minutes at room temperature on shaker with diluted secondary antibodies (150µl/well) (Table2.2). Wells were covered from this step to protect light sensitive secondary antibodies. Incubation with secondary antibodies was followed by 6x5 minutes washing using PBS (200 µl/well) in 6x5 min. Nuclei was stained using DRAQ 5 (100µl/well) nuclear stain diluted 1:1000 in PBS and followed by incubating at room temperature for 10 minutes. Stained cells were washed once in PBS (200) µl and stored in 400 µl PBS at 4^{o}C.

Table 2.1: Primary antibodies for confocal microscopy

Antigen	Primary antibody	Manufacturer	Dilution
NOS2	Rabbit	Millipore, USA (#ABN26)	1:1000
Arginase	Chicken	Millipore, USA (#ABS535)	1:1000

Table 2.2: Secondary antibodies for confocal microscopy

Secondary antibody	Manufacture	Dilution
Goat anti-rabbit IgG- Alexa 555	Life technologies, USA (#A-11034)	1:5000
Goat anti-chicken IgG- Alexa 488	Life technologies, USA (#A-11030)	1:5000

2.8.3 Imaging

Detection on the Zeiss confocal florescent microscope (figure2.1) was performed using ZEN 2012 (blue edition) with identical adjustment.

2.9 Immunofluorescence Staining

Near-Infrared (NIR) Immunofluorescence (IF) is used in pathology in order to detect and localize antigens in formalin fixed paraffin embedded (FFPE) slides. NIR florescent dyes with the defined absorption and emission wavelength in the near infrared spectra between 680 and 800 nm are used. It can be applied for multicolor imaging. In indirect IF, a primary antibody that is specific for the molecular of interest is used. A secondary antibody which is tagged to IR680/800 (Florescent dye) binds to the antigen of interest. This technique is more sensitive compared to direct immune florescence, and there is also an amplification of the signal due to the attachment of more than one secondary to each primary antibody. This technique enables quantitative analysis by using Odyssey infrared imager.

Stained sections of 67NR and 66CL4 primary tumors were also analyzed by Zeiss confocal florescent microscope based on Abcam protocol by using secondary antibodies that can be detected in the visible light spectra.

2.9.1 Preparation of tumor Sample Sections

The Leica RM 2235 microtome was used to prepare sections from 66cl4 and 67NR primary tumor tissue blocks (paraffin embedded tumor sample). Tissue blocks were kept on the ice one hour before cutting and after cutting 10 sections from the block. Thickness was set to 4 µm. Sections were placed in the 42^{o}C water bath immediately. Stretched sections were placed on the superfrost glass slides and kept in a 60^{o}C incubator for 25-30 minutes. Fixed sections were stored in -20 for later staining.

2.9.2 Pre-treatment of sections

Tumor slides were incubated at 65^{o}C for 10 minutes in order to remove paraffin as paraffin can interfere the staining. Then they were incubated 2x5minutes in xylol. Slides were rehydrated in absolute, 96% and 80% ethanol. So Slides were immersed shortly 3-5 times in each ethanol concentration. Afterwards slides were rinsed with cold running tap water for 3-5 minutes.

Dako Retrieval Solution with pH 9 was diluted by adding 325ml dH2O to 35mL 10x Dako stock solution. Retrieval reagent procedure improves deparaffinization, rehydration and specific antibody binding. Dako buffer was boiled by jet stream microwave while slides were pre-warmed in water tap at the same time. Slides were placed in the buffer while it was boiling and they were boiled together for 10 minutes using jet stream. Afterwards slides were cooled

down in cold running tap water for 30 minutes. Cooled slides were blocked with 500µl blocking buffer dilution for 40 minutes. Blocking buffer boosts sensitivity of the technique and improve signal to noise, was prepared by mixing 1:1 odyssey blocking buffer with TBST. TBST was made of Tris buffered saline (TBS) with 0.1% Tween-20.

For blocking tissue samples that were analyzed with confocal microscope, slides were blocked with 10% Bovine serum albumin (BSA) in TBST. Subsequently, slides were placed in the humidity slide box while it was on the top of the container filled with hot water. Two straight lines were drawn on the outer border of the tissue sections with Dako pen to reduce the volume of the blocking buffer and the antibody dilutions and avoid drying out the slides

2.9.3 Staining of the Sections

Blocking buffer was removed and primary antibody solution (100µl/slide) was applied. Dilution series for primary antibodies were prepared by in blocking buffer for optimizing dilution of primary antibodies (1:50, 1:100 and 1:200) (Table 2.3.). For samples that were analyzed with confocal microscope, primary antibodies were diluted in 1% BSA in TBST (Table2.4.). For negative control respective section was incubated with blocking buffer instead. Simport humidity slide box was used for incubation of slides that was filled with dH2O to reduce dryness. Incubation of slides with primary antibodies for 16 hours at 4 degree was followed by 4x 5minutes washing with TBST while samples that were analyzed with confocal microscope were washed 4×5minutes with TBS.

Odyssey Li-COR secondary antibodies were diluted 1:1000 with 1:1 Odyssey Blocking Buffer with TBS (table2.3) while confocal secondary antibodies were diluted 1:5000 in TBS (table 2.5). Slides were incubated for 40 minutes in the dark humidity box at room temperature while it was placed on a sink full of hot water in order to avoid dryness and dye bleaching. Diluted secondary antibodies (100µl/slide) were applied. Slides were located in a dark place from this step.

Slides were wash 4x 5minutes with TBS since tween can increases the background. Then stained sections were mounted with a drop of vectashield mounting medium containing Dapi and covered with coverslip. Slides were stored in the darkness at 4 degree until vectashield hardness.

Table2.3: Antibodies for NIR Immunofluorescence staining

Antigen	Primary antibody	Manufacturer	Odyssey Li-COR secondary antibody
Arginase-1	Chicken	Millipore(#ABS535)	Chicken 800 nm
NOS2	Rabbit	Millipore(#ABN26)	Rabbit 680 nm

Table 2.4: Primary antibodies for confocal microscopy

Antigen	Primary antibody	Manufacturer	Dilution
CD68	Rat	AbD serotec, USA (#MCA1957)	1:50
GFP	Rabbit	abcam, UK (#ab290)	1:200

Table 2.5: Secondary antibodies for confocal microscopy

Secondary antibody	Manufacture	Dilution
Goat anti-rat IgG- Alexa fluor,555	A-21434, Life technologies, USA	1:5000
Goat anti-rabbit IgG- Alexa fluor,488	A-11034, Life technologies, USA	1:5000

2.9.4 Scanning of the Sections

Slides were scanned using Odyssey CLx infrared imaging system that can detect the florescent dye attached to the secondary antibody. Image Studio software was used for analyzing images with the setting that is mentioned in table2.6. Slides that were stained based on Abcam protocol for confocal microscopy analysis were monitored using Zeiss confocal florescent microscope and ZEN 2012 (blue edition) with identical adjustment.

Table2.6: Image Studio setting for scanning Sections

Intensity	800 8.0
	700 6.0
Focus offset (f)	1.0 mm
Quality(Q)	Highest
Resolution(R)	21µm

2.10 Western Blot analysis

In western blot, also called immunoblotting, denatured proteins are separated based on their size. Proteins are either positive or negative charged based on their amino acid composition. In this technique, DL-Dithiothreitol (DTT) is applied as a reducing agent to disrupt tertiary conformation of proteins by reducing disulfide bands. DTT also distribute negative charge evenly on proteins. Polypeptides migrate from negative anode to positive cathode using power supply. Therefore, smaller proteins migrate faster. Polypeptides are separated using a polyacrylamide gel which isfollowed by transferring to a PVDF membrane. Appropriate gel was selected based on the well and pore size. Blotted membrane was stained by using antibody of protein of interest. A standard ladder (Odyssey two-color protein molecular weight marker) was used determining weight of the protein of interest.

2.10.1 Protein concentration measurement

Cells were counted by using Z1 Beckman cell and particle counter. Appropriate amount of cells were seeded in 6cm dishes or in a six-well plate (9.5 cm^2). Cells were treated by desired compound with appropriate concentration after cells attachment to the surface at relevant time points. Medium movement from the dishes/plates was followed by washing twice with PBS. Cell extract was made by adding 40µl 8M urea lysis buffer to six-well and 80 µl to 6cm dish followed by scraping the cells from the surface. Lysis buffer was composed by adding urea (8M), Triton-X, dithiothreitol (DTT) (reducing agent), protease inhibitor (25x complete) and phosphatase inhibitors (PIC2 and PIC3) as indicated in the table 2.7.

Table2.7: Urea lysis buffer components and concentrations

8 M Urea LB	**Concentration**	**In buffer**	**500 µL**
Urea	60,06 g/mol	8 M	410 µL
Triton-X	100 %	0,50 %	
DTT	1 M	0,1 M	50 µL
25x complete	25 X	1 X	20 µL
PIC2 (cold)	100 X	2 X	10 µL
PIC3 (cold)	100 X	2 X	10 µL

Suspension was transferred to a 1.5 ml eppendorf tube and mixed by vortexing 3×15 seconds. Non-protein components were pelleted by centrifugation for 15 minutes, 15 000 g, at 4°C. Supernatant was transferred to a new eppendorf tube. Protein extract was cryopreserved with liquid nitrogen and stored at -80°C.

Protein concentration of the extracts was measured by using Bio-Rad Protein Assay. Bio-Rad Protein Assay solution Bio-Rad Protein Dye Reagent Concentrate was diluted 1:5 with MiliQ water. Samples were diluted 1:1000 with the Bio-Rad solution and urea lysis buffer was used as a blank instead of protein. Samples were mixed by vortexing and left at room temperature for 10 minutes. Sample absorbance was measured by using a spectrophotometer (Shimadzu) at 595nm. Protein concentration was calculated in µg/µl with the equation below:

$$Protein\ concentration\ [\mu g/ml] = OD595\ mean\ value\ \times 22 \times dilution\ factor/100$$

2.10.2 Gel electrophoresis

Running buffer was made by adding 950ml deionized water (dH2O) to 50ml 20xMOPS SDS running buffer. Protein samples were diluted according to measured protein concentration in 10mM Tris-HCl (pH 8.0) in order to make equal protein concentration in all samples. Sample buffer was prepared by adding 4xLDS sample buffer to 1M DTT. Then samples were placed in an 80°C heating block for 10 minutes. Odyssey ladder IR Dye 4000 was diluted in loading mix that was prepared by adding 4xLDS to 10mM Tris-HCl (pH 8.0).

Proteins were separated using premade 10%, 12% or 4-12% polyacrylamide gel. Electrophoresis gel- cassette was placed in the Xcell SureLock Mini-cell. Running buffer was added to the cassette. Equal amount of protein samples were loaded to the wells. For protein separation 200 volts (V) was applied for 60 minutes.

2.10.3 Membrane transfer using XCell II blotting system (Wet transfer)

Separated proteins were transferred to a PVDF membrane (pore size is 0.45 µm, >20 kDa). Membrane was hydrated in methanol, rinsed in dH2O and placed in transfer buffer before use. Transfer buffer was made by adding 425ml dH2O to 25ml 20xTransfer buffer and 50ml methanol. Blotting pads were also placed in transfer buffer before use. Afterwards, membrane was placed on the top of the gel, surrounded by filter papers and blotting pads (Figure2.3). Proteins were transferred at 30 V for 90 minutes.

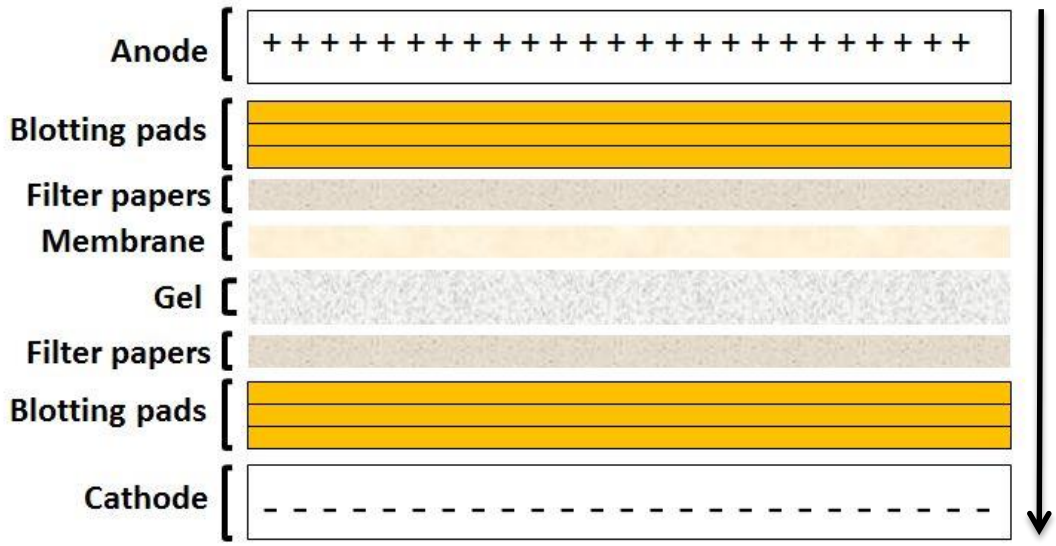

Figure 2.2: Schematic wet blot transfer system. Proteins transfer from gel matrix to nitrocellulose membrane using wet (Tank) transfer in the "transfer sandwich". This system is pressed together using Xcell SureLock Mini-cell and placed vertically in a tank between steel/platinum wire electrodes (cathode and anode) and filled with transfer buffer. Electrical flux from anode to cathode results in protein transfer from gel to the membrane. This system is placed in the ice pack or at 4°C (illustration by author).

2.10.4 Membrane blocking and immunostaining

For preparing blocking buffer the same volume of Odyssey blocking buffer was added to TBST. Membrane was blocked for one hour at room temperature on a roller plate at 50rpm. Primary and secondary antibodies were diluted in blocking buffer. Membrane was stained with primary antibody (Table 2.8) overnight at 4°C on a roller plate at 50rpm, and with secondary antibody (Table 2.9) for one hour at room temperature on a roller plate at 50rpm. After staining with primary antibody membrane was rinsed with TBST 3x10minutes, after staining with secondary antibody it was washed with TBS 3x10minutes. All membrane were stained for ACTB as a loading control.

Proteins were detected using Odyssey CLx infrared imaging system and Image Studio software.

Table 2.8.Primary antibodies for western blot staining

Antigen	Primary antibody	Manufacturer	Dilution
β-actin	Mouse	abcam, UK (#ab6276)	1:1000
iNOS	Rabbit	Millipore, USA (#ABN26)	1:1000
Arginase-1	Chicken	Milllipore, USA (#ABS535)	1:1000
Arginase	Goat	abcam, UK (#ab60176)	1:1000

Table 2.9.Secondary antibodies for western blot staining

Secondary antibody	Manufacture	Dilution
Goat anti- mouse IgG- IRDye 680	LI-COR Bioscience, USA (#926-68070)	1:20.000
Goat anti-rabbit IgG- IRDye 680	LI-COR Bioscience, USA (#926-68071)	1:5000
Goat anti-rabbit IgG- IRDye 800	LI-COR Bioscience, USA (#926-32211)	1:5000
Donkey anti-chicken IgG- IRDye 800	LI-COR Bioscience, USA (#926-32218)	1:5000
Donkey anti-goat IgG- IRDye 680	LI-COR Bioscience, USA (#926-68074)	1:5000

2.11 Quantification of mRNA gene expression using Real-time PCR

Quantitative Real-time polymerase chain reaction (RT-qPCR) quantifies a specific nucleic acid sequence by detecting and measuring amount of mRNA in a given sample, generating copies of the template nucleic acid sequence and measuring emitted florescence during each cycle that is proportional to the amount of PCR product. The cycle that the PCR product is first detected (Ct value) can be determined using step one Real-time PCR system. For this procedure cells were co cultured with different co culture techniques used and RNA was isolated. RNA was converted to cDNA and cDNA was amplified and measured expression of mRNA was quantified (122).

2.11.1 Cell stimulation and culturing

Conditioned medium from 66cl4 and 67NR

RAW 264.7 cells were counted using Z1 Beckman cell and particle counter. Appropriate number of cells were seeded in a 6cm dishes or a six-well plate (9.5 cm^2). Cells were placed in an incubator for approximately 4 hour. Attached cells were treated by desired compound (IFN-γ and LPS or IL4) or conditioned medium of 66cl4 and 67NR with needed concentration at relevant time points. Appropriate amount of 66cl4 and 67NR cells were seeded as untreated control. After incubation for 1-2 days medium was removed and cells were harvested. RNAprotect cell Reagent was added to the six-well plates (500µl/well) and to 6cm dishes (1000 µl). Detached cells were transferred to RNase-free tubes and stored at 4^{o}C.

Cultivation in transwells

Appropriate medium was pipetted to both lower and inside compartment of the six-well plate transwells. Incubation for 1-2 hours was followed by medium removement. Desired number of RAW 264.7 cells was seeded in lower part of wells while 67NR and 66cl4 cells were seeded in the upper wells. Cells were incubated for 2-3 days. Medium was then removed from both lower and upper compartments and cells were harvested using 500µl RNAprotect Cell Reagent. Detached cells were transferred to RNase-free tubes and stored at 4^{o}C.

2.11.2 RNA isolation

RNA was isolated based on Qiagen RNAprotect Cell Reagent Handbook protocol 2010 (123). Cells were disrupted by using RLT Plus buffer supplemented in the kit. RLT buffer was

prepared by adding 10µl β-mercaptoethanol (β-ME) per 1ml RLT Plus buffer. β-ME can help to avoid RNA degradation during RNA purification while RLT buffer lysis the membrane. Cells were separated from the buffer using RNeasy spin column and subsequent centrifugation. RW1 buffer was used for washing the samples. Centrifuged column membrane was washed with RPE Buffer diluted in ethanol according to the manufacturer. Residual ethanol interferes with downstream reactions; therefore, it should be removed completely.

2.11.3 Concentration measurement

Optical density (OD) was measured using NanoDrop Spectrophotometer which is capable of measuring nucleic acid concentration in the higher concentrated samples than standard cuvette spectrophotometer at 260-280 and 260-230 nm. Based on Thermo Fisher Scientific protocol 1µl of sample was pipetted onto the end of fiber optic cable on the instrument and concentration was measured using ND-1000 software (124). Instrument calculates RNA purity and sample concentration based on Beer's Law (ng/µl) using 220/280 and 260/230 nm. OD ratios of samples at 260/280 nm should be 2.0 or more to be accepted as a pure RNA and 1.8-2-2 for 260/230 nm. This ratio is trustable and this RNA is not contaminated. Lower ratio can be due to the protein or other contamination. OD of samples used in this project were more than 2. Samples were stored at -80^{o}C.

2.11.4 cDNA synthesize and RT-qPCR

RNA samples were diluted in RNase-free water to a concentration of 250ng/µl to a total volume of 5µl. cDNA was synthesized using Qiagen QuantiTect Reverse Transcription Kit according to the manual (125). Genomic DNA elimination reaction master mix was prepared by mixing appropriate volumes of gDNA Wipeout buffer to template RNA and RNase-free water based on Qiagen protocol (Table2.10).Master mix was incubated 2minutes at 42 degree using thermal cycler. No-script reverse transcriptase and no-RNA template controls were included to ensure that all genomic DNA (gDNA) is removed. No-RNA template contains 2µl one of RNase-free water and no-script reverse transcriptase sample contains 2µl of one of the samples.

Table 2.10: DNA elimination reaction mix components

Component	Volume/reaction
gDNA Wipeout Buffer, 7x	2µL
Template RNA (250ng)	2µL
RNase-free water	10µL
Total volume	14µL

Adequate volume of reverse-transcription master mix was prepared (Table 2.11). Reverse-transcription master mix (6µl/well) was added to the respective template RNA (14µl/well). Incubation of samples for 15minutes at 42ºC was followed by 3minutes incubation at 95ºC using thermal cycler in order to inactivate Quantiscript Reverse Transcriptase. Produced cDNA was stored at -20°C.

Table2.11. Reverse-transcription master mix components

Components	Volume (1x)µl
Quantiscript Reverse Transcriptase	1µl
Quantiscript RT Buffer (5x)	4µl
RT Primer Mix	1µl
Total volume	6µl

QuantiTect Primer Assays and QuantiTect SYBR green PCR kit from Qiagen were used (Table 2.12). Samples were diluted 1:5 using dH_2O to get 10ng total cDNA concentration. Diluted samples were mixed and 5ng/µl or 25ng/µl of the respective cDNA was loaded (volume of the cDNA added should not exceed 10% of the final PCR volume). Reaction master mix was prepared (Table2.13). Mixed reaction master mix was dispensed into PCR plates (23µl/well) and respective cDNA was added. PCR plate was centrifuged for 2minutes at 1500 rpm before RT-PCR program running based on Qiagen protocol (Table2.14). Melting curve was set on 65°C for 1 minute to 95 °C for 1 minute.

Table 2.12: RT-qPCR QuantiTect Primer Assays

Quantitect Primer Assay	Manufacture
NOS-2	Qiagen, Netherland (#QT00100275)
CD163	Qiagen, Netherland (#QT00123074)
Li	Qiagen, Netherland (#QT00163646)
Arg1	Qiagen, Netherland (#QT00134288)
Hmbs	Qiagen, Netherland (#QT00494130)
Hprt	Qiagen, Netherland (#QT00166768)

Table2.13: Reaction mix components

Component	Volume per reaction for 5ng/µl	Volume per reaction for 25ng/µl
2x QuantiTect SYBR Green PCR master mix	12,5 µl	12,5 µl
10x QuantiTect Primer Assay	2,5 µl	2,5 µl
RNase free water	8µl	-
Cdna	2	10
Total volume	25 µl	25 µl

Table2.14: Quantitative RT-PCR program on step one real time system

PCR initial activation step	15 minutes	95°C	Taq DNA polymerase activation
Denaturation	15 seconds	94°C	
Annealing	30 seconds	55°C	
Extension	30 seconds	77°C	Data collection
Number of cycles	35-40		Depends on amounts of target cDNA and abundance of the target

2.11.5 Statistical analysis (relative quantification)

Ratio of target gene was determined using relative quantification (fold difference). Therefore, samples fold differences was calculated using an untreated sample as calibrator and an endogenous reference gene (housekeeping gene) as normalizer. Primers efficiency was calculated in the group and was included in the data analysis based on Pfaffl method described by manufacture. Fold induction and standard deviation was calculated using excel. Significancy of the obtained results were analyzed using t-test's statistical significance in Prism 6 (GraphPad).

2.12 TaqMan SNP genotyping

TaqMan SNP genotyping assay is known for its sensitivity and ease of use and is widely used for detection of polymorphisms within different organisms. The prominent difference between this assay and other PCR methods is the utilization of sequence specific oligonucleotide fragments called "GMB Probes". The opposite extremities of the probes are bind to a quencher molecule and a reporter molecule. TaqMan primers hybridize to the origin uphill a SNP while GMB probes are complementary to the sequence containing the SNP of interest. Florescent signal production because of the reporter/quencher cleavage leads to the detection of SNPs (Figure2.3) (126). In this project TaqMan SNP genotyping was used in order to investigate heterogeneity of 66cl4 and 67NR primary tumors and calculating percentage of non-tumor cells within each tumor.

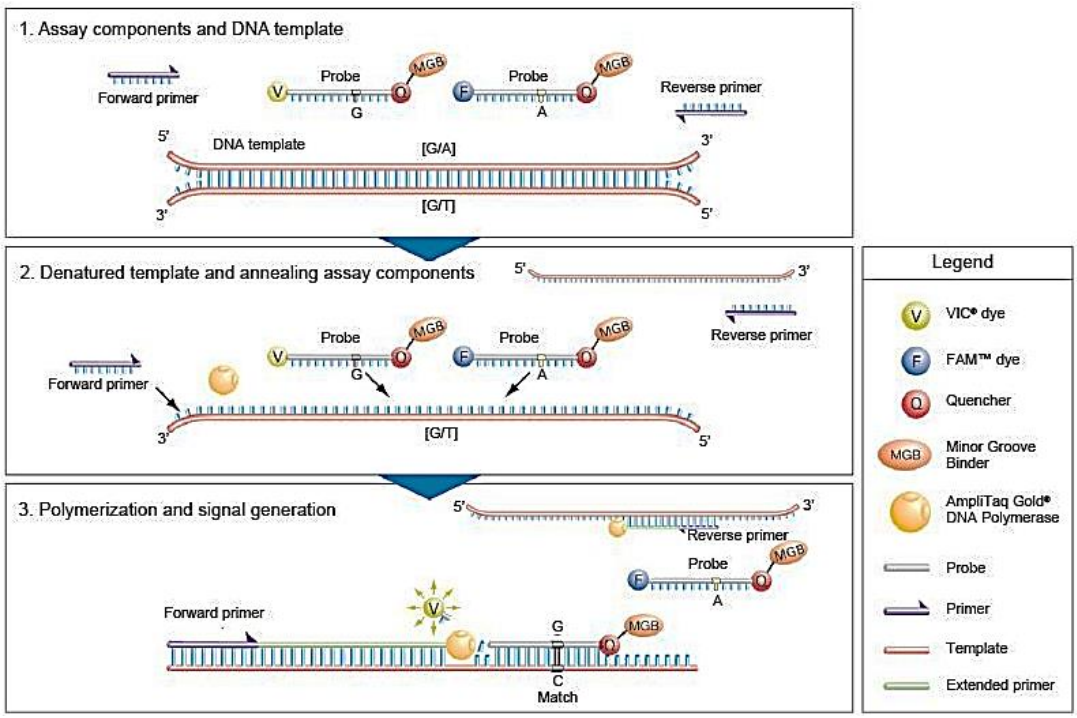

Figure2.3: TaqMan SNP Genotyping principle. TaqMan primers and probes are able to hybridize to the targeted SNP site. In this reaction primers are complementary to the DNA sequence and will extend due to the 5´ nuclease activity of AmpliTaq Gold DNA Polymerase. Probes are bind to a reporter and a quencher. Their cleavage due to the PCR amplification produces a florescent signal (126). In this assay one of probes detect wild type allele and the other one detect mutated allele

2.12.1 Experiment designing

BALB/cfC3H blood, 66cl4 cancer cell line, 67NR cancer cell line, 66cl4primary tumor and 67NR primary tumor have already been exome sequenced in Bjørkøy group. The genetic variation of these samples and the created list of genetic variations has been checked and

assessed. Exome sequencing data revealed six SNPs that are homozygous in both 66cl4 and 67NR but are not present in BALB/cfC3H blood. Primers and probes were ordered and designed according to the Applied Biosystems handbook (127). Homozygous mutations identical in both 66cl4 and 67NR cancer cell lines that does not exist in BALB/cfC3H mouse were identified. NCBI on line database (BLAST) was used to identify the most unique sequences. Sequences was sent to Applied Biosystems company and they investigated flanking sequences around these mutations for primer designing. Data regarding sequence of the chromosome can be seen in the appendix II.

2.12.2 DNA extraction

DNA was extracted and purified from BALB/cfC3H mouse blood, Raw 264.7 cells, 66cl4 and 67NR primary tumors and cell lines based on Qiagen Genomic DNA handbook 2012 (128). DNA concentration was measured using NanoDrop based on Thermo Fisher Scientific protocol. Instrument calculates DNA concentration (ng/µl) using absorbance ratio at 220/280 and 260/230 nm. OD ratios of samples at 260/280 nm should be 1.8 or more and 1.8-2-2 for 260/230 nm. DNA samples were stored at -80^{o}C (see 2.11.3).

DNA extraction from cultured cells and blood

DNA from 66cl4, 67NR and RAW264.7 cells and BALB/cfC3H mouse blood lymphocytes was extracted. Cells were washed with PBS, detached from the flask using PBS-0.02% EDTA/trypsin and resuspended in respective medium. Cells were washed twice with PBS and centrifuged 5 minutes at 1500 rpm before, after and in between washings. Cell pallet was dissolved in 500µl PBS.

DNA from all samples was purified by loading samples in Genomic-tip 20/G. The tips were washed with buffer QBT before loading and buffer QC after loading the samples. Samples go through the Genomic-tip by gravity flow. Genomic DNA was eluted using buffer QF and participated by adding isopropanol. Samples were mixed and centrifuged immediately at 5000 g for at least 15 minutes at 4^{o}C. DNA pellet washing with cold 70% ethanol was followed by Vortexing and centrifugation at 5000 g for 10 minutes at 4^{o}C. Pellet was air dried and resuspended in 100µl of 10mM Tris-HCl (pH 8.5).

DNA extraction from primary tumor samples

DNA was extracted from 20 mg of 66cl4 and 67NR primary tumor tissue using G2, QC, and QF buffers that are supplemented in the kit. Tissue samples were homogenized adding bulck beads and QIAGEN Proteinase K solution. After 2 hours incubation at 50°C clear lysate was loaded in QIAGEN Genomic-tip 20/G which was equilibrated with QBT buffer. The procedures that follows are identical to that exposed in the previous paragraph.

2.12.3 TaqMan SNP genotyping assay

For standard curve assessment, DNA of 66cl4 and RAW264.7 macrophage cell lines were mixed with different percentages (Table3.2). Then these samples were genotyped. In other experiments DNA samples were diluted in dH_2O to a concentration of 1ng/µl to a total volume of 100µl. Reaction master mix was prepared (Table2.15) based on Applied Biosystems handbook using TaqMan genotyping master mix and custom designed probes and primer assays. Reaction master mix was dispensed into PCR plates (15µl) and DNA was added (10µl). TaqMan genotyping PCR program was set up on step one real time system using Step one software version 2.3 (Table2.16).

Table2.15: Reaction master mix components

Reaction component	**Volume/well (µl)**
TaqMan genotyping master mix (2x)	12,5
40x Assay Mix	0,625
dH_2O	1,875
Total Volume	15

Table2.16: TaqMan genotyping PCR program on step one real time system

Pre PCR(Holding stage)	30 seconds	60°C	Data collection
Denaturation	10 minutes	95°C	
Annealing	15 seconds	92°C	
Extension	1 minutes	60°C	
Number of cycles	40		
Post read(Holding stage)	30 seconds	60°C	Data collection

2.12.4 Statistical analysis

Percentage of tumor and non-tumor cells was estimated by assessing allele 1 and 2 frequency. This experiment was designed based on 66cl4 and 67NR (mutated allele) and BALB/cfC3H blood (wild type allele). Analysis demonstrated that RAW264.7 macrophages have the wild

type allele. In addition, little amounts of DNA from BALB/cfC3H blood was available. Therefore, for creating standard curve, DNA of RAW264.7 cells was used instead of BALB/cfC3H blood. For creating standard curve, DNA of 66cl4 and RAW264.7 were mixed with different percentages. 2'-chloro-7'-phenyl-1,4-dichloro-6-carboxyfluorescein (VIC)-labeled probes detected wild type alleles (allele1), and 6-carboxyfluorescein (FAM)-labeled probes detected the mutated alleles (allele2). Allele1 and allele 2 ΔRn values were extracted from step one software. Rn is the fluorescence of the reporter dye divided by the fluorescence of a passive reference dye (ROX) while ΔRn is Rn of post-PCR read minus Rn of pre-PCR read. ΔRn of samples for allele 1 was relatively calculated using 66cl4 allele1 ΔRn as calibrator. ΔRn of samples for allele 2 was relatively calculated using RAW264.7 allele 2 ΔRn as calibrator. For example:

1) $Relative\ allele\ 1\ \Delta Rn\ for\ 100\%66cl4 = 100\%\ 66cl4\ allele\ 1\ \Delta Rn - 100\%\ 66cl4\ allele\ 1\ \Delta Rn$

2) $Relative\ allele\ 1\ \Delta Rn\ for\ 90\%66cl4 + 10\%RAW264.7 = 90\%66cl4 + 10\%RAW264.7\ allele\ 1\ \Delta Rn - 100\%66cl4\ allele\ 1\ \Delta Rn$

Average percentage of tumor cells was estimated based on both allele 1 and allele 2 (Figure2.4). For example:

1) $Percentage\ of\ RAW264.7\ cells\ in\ the\ 100\%66cl4\ based\ on\ allele1$

$$= \frac{100\%66cl4\ relative\ allele1\Delta Rn}{100\%\ RAW264.7\ relative\ allele1\ \Delta Rn} \times 100 = 0$$

2) $Percentage\ of\ RAW264.7\ cells\ in\ the\ 90\%66cl4 + 10\%RAW264.7\ based\ on\ allele1$

$$= \frac{90\ \%66cl4 + 10\%\ RAW264.7\ relative\ allele1\Delta Rn}{100\%\ RAW264.7\ relative\ allele1\ \Delta Rn} \times 100$$

Then percentage of RAW264.7 cells in the samples was calculated based on allele 1 and afterwards percentage of tumor cells in each sample was calculated based on percentage of RAW264.7 macrophages (Percentage of tumor cells= 100 - percentage of RAW264.7). R-squared value (R^2) for the standard curve was calculated using excel file. R^2 value varies between o and 1 and represents how close the data are to the fitted regression line (R^2=

Explained variation / Total variation). The closer the R-squared is to 1 the better the model fits the data.

In next experiments DNA samples from 66cl4 cultured cells, 67NR cultured cells, BALB/cfC3H mouse blood, 66cl4 and 67NR primary tumors were genotyped. Based on results from experiment 1 (standard curve), frequency of alleles in these experiments was calculated using allele 1. As mentioned, ΔRn values of samples was used for relative calculation of tumor cells in tumor samples. Standard deviation (SD) was calculated using excel.

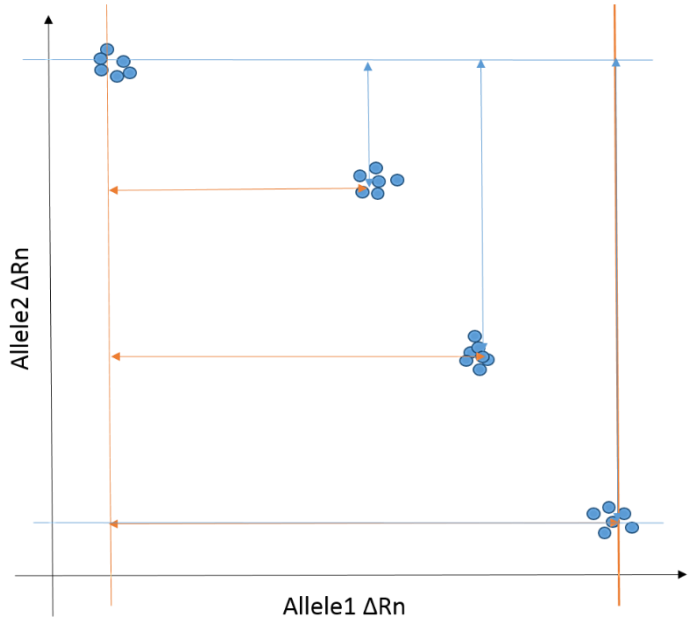

Figure 2.4: Average percentage of tumor cells based on allele 1 and allele 2
For statistical analysis, percentage of tumor cells were calculated based on both allele 1 and allele2. First percentage of 66cl4 cells in the samples was calculated based on allele 2 (red). Then percentage of RAW264.7 cells in the samples was calculated based on allele 1 (blue) and afterwards percentage of tumor cells in each sample was calculated based on percentage of RAW264.7 macrophages (Illustrated by author).

3. Results

3.1 The more heterogeneous appearance of 66cl4 primary tumors is due to higher numbers of infiltrating cells

Tumors are unique regarding microenvironment (22). Microenvironment composition can affect primary cancer growth, invasion and metastasis (21). This study was focused on the differences in cellular constitution and presence of macrophages in primary tumors of the mammary carcinoma cell lines 66cl4 and 67NR. Presence of more infiltrating cells, macrophages in particular, might contribute to more aggressive growth of 66cl4 primary tumor. Therefore, the first step was to determine if other cellular subpopulations exist in the primary tumors of 66cl4 and 67NR other than tumor cells. Comparing different status of infiltrated cell in 66cl4 (metastatic) to 67NR (non-metastatic) can give information about role of different infiltrated cells within primary tumors.

3.1.1 Non-tumor cells can be present at primary tumors of 66cl4 and 67NR

Previously, cultured cells, primary tumors of 66cl4 and 67NR as well as 66cl4 metastasis have been RNA sequenced in the Bjørkøy group. Transcriptome data represents information regarding cell types that can present in the primary tumors. Literature suggests different genes and proteins as cell specific markers. Markers of different cells that can be present in the tumors were chosen and summarized in table I (see appendix). Assessing both transcriptome data and literature can be used to indicate the presence of other cell types than tumor cells by comparing specific genes in the cells and tumors. Differences in mRNA expression level of stromal and immune cell markers in cell lines and primary tumors were compared (Table 3.1). Low mRNA expression in the breast cancer cells and higher expression in the primary tumors represents possible infiltration of the related cell type in the primary tumor. For instance, Cd68 has been used as a macrophage marker in several studies. Higher expression of Cd68 in primary tumor samples than cell lines suggests possible infiltration of macrophage within the primary tumors. It can also be used as a suitable marker for comparing macrophage infiltration in this model. Emr1- another macrophage marker- is not expressed in both cell lines and is similarly upregulated in both primary tumors.

Arginase1 (ARG1) is a known marker for M2 macrophages. Analyzing transcriptome data reveals low expression of this marker in breast cancer cells and 67NR primary tumor and higher

expression mRNA level of Arg1 in 66cl4 primary tumors. Cd74 is another macrophage marker that is highly upregulated in both primary tumors than cancer cells. This result can be due to the higher infiltration of M2 macrophages in 66cl4 primary tumor than 67NR. This is supported by assessment of other macrophage marker candidates. However, probably there are more macrophage markers that can be analyzed in transcriptome data.

Vimentin (Vim) - a well-known marker for fibroblasts- was expressed high in both cell lines but only expressed in one 66cl4 primary tumor. Due to this difference, further investigation regarding role of vim in primary tumors can be interesting. However, vimentin is highly expressed in the cell cultures of pure 66cl4 and 67NR and cannot be used as an indicator of fibroblast in this model.

Generally, transcriptome data analysis demonstrates higher macrophage marker related mRNA expression in the primary tumor of 66cl4 and 67NR than tumor cells. It can be due to the infiltration of macrophages within primary tumors. In addition, analysis demonstrated similar expression of M1 macrophage markers in both 66cl4 and 67NR primary tumors. However, estimating number of infiltrated cells needs further investigation by other methods.

Table 3.1: Transcriptome Data Analysis. Markers and mRNA expression level of stromal cells in the tumor microenvironment
Cell66cl4_V: Average expression value of the replicates from Cell line 66cl4. **Cell67NR_V:** Average expression value of the replicates from Cell line 67NR. **Vitro_pvalue:** Adjusted p-value from t-test on the comparison of expression values of the replicates of Cell66cl4_V and Cell67NR_V. **Primary66cl4_V:** Average expression value of the primary tumors from 66cl4. **Primary67NR_V:** Average expression value of the primary tumors from 67NR. **Vivo_pvalue:** Adjusted p-value from t-test of the comparison of primary tumors from 66cl4 and 67NR

Cell type	Gene	66cl4 Cell line _V	67NR Cell line _V	Vitro _p value	66cl4 Primary tumor_ V	67NR Primary tumor_ V	Vivo _p value
Macrophages general marker	Cd68	1,36905	5,08001	0,0001156	182,48	96,8061	0,0001985
	Emr1	0,0198353	0,0159229	1	60,9174	67,5694	0,350149
M1 Macrophages	Fcgr1	0,0274622	0,0474556	1	35,1767	38,2861	0,46828
	Nos2	0,101048	0,001711	1	1,5577	2,04159	0,178111
	Cd40	0,0313455	0,01	1	4,52739	4,34538	0,868842
	Cd80	0,357589	0,913047	0,0001156	3,55156	3,61519	0,947027
	Cd74	0,746012	0,44891	0,0193102	435,416	898,108	0,0001985
M2 Macrophages	Cd163	0,0195665	0,0029088	1	32,8626	7,59919	0,0001985
	Arg1	0,00847143	0,00906541	1	114,616	0,191906	0,0001985
	Mrc1	0,125848	0,096672	1	202,967	113,804	0,0001985
B cell	Cd300lg	0,01	0,01	1	5,17632	6,78337	0,100145
	Cd300a	0,0173552	0,0791101	1	4,78531	7,32302	0,0003761
T cell general marker	Cd3e	0,0091694	0,01	1	1,23928	4,64167	0,0001985
	Cd3d	0,0239321	0,01	1	1,7272	4,32501	0,0018929
	Cd3g	0,0200508	0,00717778	1	4,3106	13,5648	0,0001985
Helper T cell	Cd4	0,0037259	0,01	1	1,51006	7,20981	0,0001985
Cytotoxic T cell	Cd8a	0,01	0,01	1	0,700704	4,56732	0,0001985
Fibroblast	Vim	1456,38	2921,7	0,0001156	2009,47	0,01	1
NK cells	Ncr1	0,0043006	0,0092422	1	4,87394	13,4194	0,0001985
Dendritic cell	Cd83	0,0057225	0,00904042	1	20,9866	15,5939	0,0107666
	Il3ra	0,01	0,01	1	3,09863	2,46223	0,386578
Endothelial Cell	Cd34	77,682	86,402	0,258236	69,9401	127,617	0,0001985
	Pecam1	0,0269223	0,0614277	1	34,3667	32,9393	0,735822
	Vcam1	0,709771	0,8733	0,159097	8,665	24,6174	0,0001985
	Cdh5	0,0390046	0,119393	1	27,916	26,3239	0,625893
Monocytes	Csf1r	0,052124	0,08567	1	164,309	120,572	0,005756
Neutrophil	Itgam	0,018483	0,02412	1	85,6426	43,5374	0,0001985

3.1.2 66cl4 and 67NR primary tumor heterogeneity is due to the presence of non-tumor cells in tumor stroma

Transcriptome data analysis suggested the presence of non-tumor cells in the 66cl4 and 67NR primary tumors. The presence of non-tumor cells can be determined by analyzing mutated and wild type allele. DNA isolated from BALB/cfC3H mouse blood, 66cl4 and 67NR breast cancer cells was previously exome sequenced. TaqMan genotyping assay was performed in order to investigate existence of non-tumor cells in the primary tumor samples. DNA sequence of 66cl4 and 67NR cancer cells were investigated in order to identify common genetic variant specially for tumor cells. Primers and probes were designed based on the identical mutations in 66cl4 and 67NR cancer cells that does not exist in BALB/cfC3H mouse. 2'-chloro-7'-phenyl-1,4-dichloro-6-carboxyfluorescein (VIC)-labeled probes detected wild type alleles (allele1), and 6-carboxyfluorescein (FAM)-labeled probes detected the mutated alleles (allele2). It was speculated that number of tumor and non-tumor cells can be estimated by calculating frequency of allele 2 and allele 1, respectively. For the first step, accuracy and sensitivity of this technique and the designed primers and probes should be analyzed. RAW264.7 cells were used is this experiment as sample that does not possess the mutant allele. The standard curve was plotted by mixing DNA of 66cl4 with increasing amount of RAW264.7 DNA ranging from 10% up to 90%. Then these samples were genotyped. As the allelic discrimination plot indicates, pure 66cl4 cultured cell DNA exhibits more homozygosity for allele 2 (A/A, FAM) and pure RAW264.7 macrophage DNA demonstrate signal for allele1 (G/G, VIC) (Figure 3.1). With increasing amount of RAW264.7 DNA, the signal for allele 2 decreased and at the same time the signal for allele 1 increased. Allele 1 ΔRn was plotted against allele 2 ΔRn. A linear regression with the high R-squared (R^2) value was observe. The closer the R^2 is to 1 the better the model fits the data. In this experiment R^2 value (0.9783) demonstrates closeness of the data to the fitted regression line (Figure 3.1).

As it has been described in material and method section (section 2.12.4), for calculating frequency of allele 1, ΔRn of each sample was quantified relatively based on 66cl4 ΔRn. For calculating frequency of allele 2, ΔRn of each sample was quantified relatively based on RAW264.7 ΔRn. Average percentage of tumor cells was estimated based on both allele 1 and allele 2 (Table3.2). The calculated percentage of the tumor cells was compared with the pipetted sample. Results from allele 1 demonstrated that the calculated percentages are closer to the actual values and a linear decrease in number of tumor cells was observed. As it can be seen in table 3.2 number of tumor cells in the sample containing 90% 66cl4 is close to sample that

contains 15% less of 66cl4 DNA. In contrary, no linear range in average number of tumor and non-tumor cells by decreasing concentration of 66cl4 DNA in samples based on allele 2 was observed. Based on these results, allele 1 seems to be more suitable for calculating percentage of nun-tumor cells.

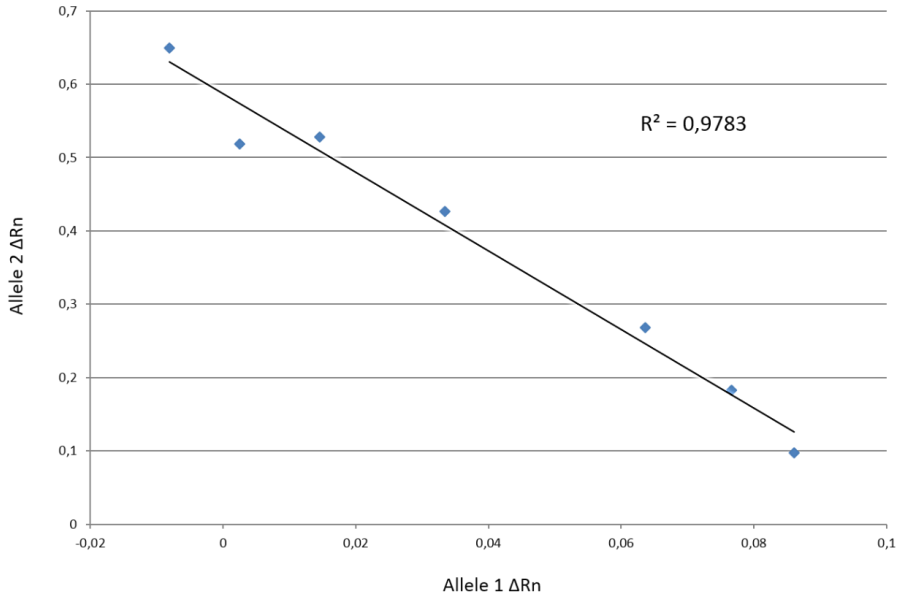

Figure 3.1: Allelic discrimination standard plot of RAW264.7 cells and 66cl4 cancer cells
Allelic discrimination plot demonstrates genotyping results from TaqMan SNP genotyping assays for eight different samples. 66cl4 and RAW264.7 cells were genotyped by analyzing mixture of 66cl4 cultured cells and RAW264.7 cells. X and Y-axis demonstrates Vic and FAM signal fluorescence values, respectively, which are used for the clustering of the samples. Therefore, 66cl4 cells that exhibits FAM signal is homozygous for allele 2 and RAW264.7 sample (VIC signal) is homozygous allele 1. Samples that are mixture of two different DNA were elevated both FAM and VIC signal. It demonstrates exhibition of both alleles in different percentage.

Table 3.2: Percentage of tumor cell average based on allele 1 and allele 2

Sample	Number of tumor cells based on allele1	Number of tumor cells based on allele2
100%66cl4	100	100
90%66cl4 +10% RAW264.7	88,71167285	76,31594178
75%66cl4 +25% RAW264.7	75,92801956	78,01868434
50%66cl4 +50% RAW264.7	55,8744944	59,61132131
25%66cl4 +75% RAW264.7	23,8833765	30,81832513
10%66cl4 +90% RAW264.7	10,0633295	15,4231007
100% RAW264.7	0	0

Data from the first experiment demonstrated that allele frequency and subsequently number of tumor and nun tumor cells can be calculated based on allele1 using ΔRn of each allele in the sample. In order to investigate cellular heterogeneity of 66cl4 and 67NR primary tumors TaqMan SNP sequencing assays were performed. For this experiment, the DNA samples from

66cl4 cultured cells, 67NR cultured cells, BALB/cfC3H mouse blood, 66cl4 and 67NR primary tumor were genotyped. Allelic discrimination plots from two different experiments demonstrate the intensity allele 2 (mutated) signal in 66cl4/67NR cultured cells and intensity of allele 1 (wild type) signal in BALB/cfC3H mouse blood (Figure 3.3). Results from experiment A demonstrated a linear range between samples using chromosome 1 primer assay. However, tumor samples in experiment B demonstrate deviation from the regression line on allelic discrimination plot. As it has been demonstrated, deviation of allele 2 was observed in the standard curve. This deviation might be due to the nonspecific binding of the probe detecting the mutated allele. Samples ΔRn was used for estimating number of tumor and non-tumor cells in the primary tumors. Results from these two experiments can suggests that ΔRn values of samples can be used for relative calculation of tumor cell/normal cell percentage in tumor sample based on allele1. Statistical analysis suggests that almost 40% of 66cl4 primary tumors and 30% of 67NR primary tumors are non-tumors cells.

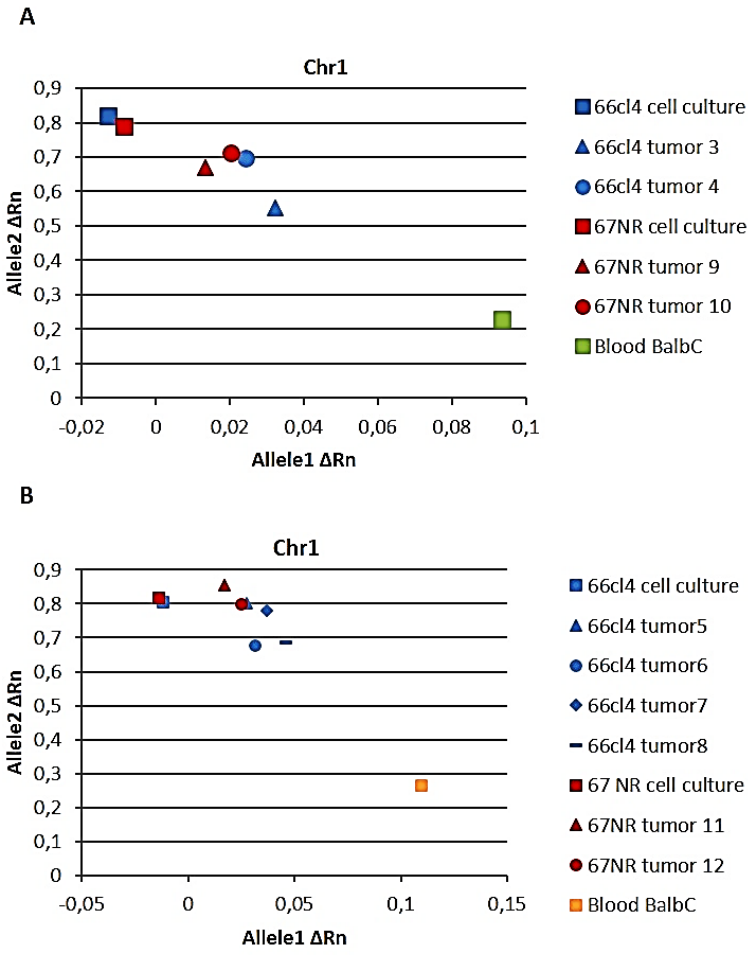

Figure 3.2: Allelic discrimination plot chromosome 1 primer assay
A) and **B)** represent allelic discrimination plot of two different experiment based on chromosome 1 probe and primer assay. This blot demonstrate ΔRn of genotypes G/G (willed type, allele 1), G/A and A/A (mutated, allele 2). VIC represents wild type on *x*-axis and FAM demonstrates mutated allele on *y* –axis.

3.1.3 66cl4 primary tumor sections are more heterogeneous than 67NR

In order to assess heterogeneity of 66cl4 and 67NR primary tumors and identify presence of infiltrated cells, pre-stained H&E sections were investigated. Formalin-fixed paraffin embedded (FFPE) sections of 66cl4 and 67NR primary tumors were stained with hematoxylin and eosin dyes. 66cl4 primary tumor sections seem more heterogeneous that 67NR (Figure 3.3). In 66cl4 primary tumor sections, a mixture of tumor cells and non-tumor cells were observed (Figure3.3A). Some cells were tagged as potential macrophages (thick arrows) with a foamy cytoplasm and a rounded nucleus. Lymphocytes (thin arrows) could be observed with round nucleus and smaller portion of cytoplasm compared to macrophages. No structure that could represent a fibroblast or a dendritic cell was identified. Nevertheless, these cell types cannot be certainly defined by H&E staining and a more precise method such as immune staining is needed.

In contrary, in 67NR primary tumor sections cells are more compact and most of the cells seems similar (Figure 3.3B). 67NR tumor sections looks less heterogeneous than 66cl4. This is in contrary with genotyping results that suggests heterogeneity in both primary tumors.

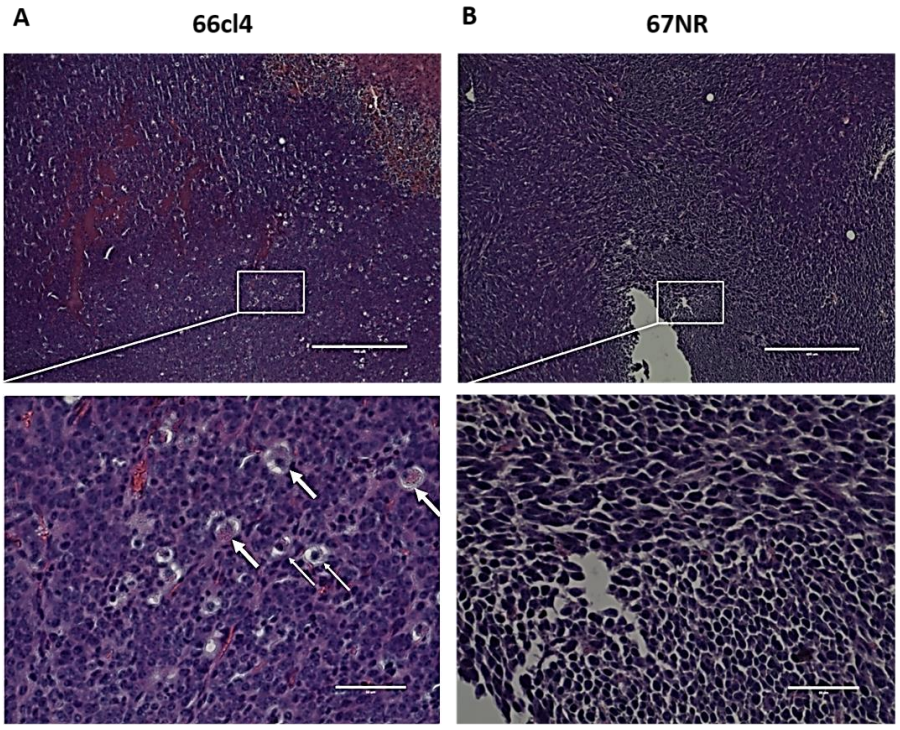

Figure 3.3: H&E stained sections of 66cl4 are more heterogeneous than 67NR
Hematoxylin is a basic dye and stains nucleus purple while eosin is an acidic dye that stains basic cytoplasm pink with eosin. Images were obtained using EVOS FL Auto Cell microscope. **A)** 66cl4 primary tumor sections seem heterogeneous(×10). Macrophages (thick arrows) with foamy cytoplasm and lymphocytes (thin arrows) with smaller cytoplasm and big round nucleus can be observed in the 66cl4 tumor section in focus (×40). **B)** 67NR tumor sections do not seem heterogeneous. No specific cell structure can be distinguished in the 67NR tumors (×10 and ×40). Right side bars in the upper images are 400 µm and in down images are 60µm.

3.2 66cl4 tumor heterogeneity can be due to the presence of polarized macrophages, M2 macrophage in particular

Results from studies in section 3.1 demonstrated higher number of non-tumor cells within 66cl4 primary tumors than 67NR. Identification of tumor microenvironment subpopulation is necessary and leads to better understanding of their function in tumor progression. Accumulated evidence demonstrates that macrophage infiltration promote metastasis of breast tumor and correlated with aggressive breast tumor behavior (96-98). Therefore, presence and polarization of macrophages in the primary tumors of 66cl4 and 67NR were investigated.

3.2.1 There is no correlation between expression of Cd68, Nos2 and Arg1 and human breast cancer patients survival

Based on literature study and by assessing transcriptome data, one M1, one M2 and a general macrophage marker were chosen for further analysis. NOS2, ARG1 and CD68 have been used in several studies as M1, M2 and general macrophage marker, respectively. In order to study correlation between mRNA expression of these genes and patient survival, Breast mark online database was used (129). Median mRNA expression of each gene in tumor grade 3 (metastatic) in general and in basal-like tumors related to disease free survival (DFS) was analyzed. In this algorithm, Pam50 category that utilizes the genes from Parker *et al*., 2009 to subtype the breast cancer samples was studied (130). There is no correlation between survival rate in breast cancer patients and low or high expression of these three genes (Figure3.4). However, these markers were used in this study as macrophage markers that can be used in different methods such as immunostaining and immunoblotting.

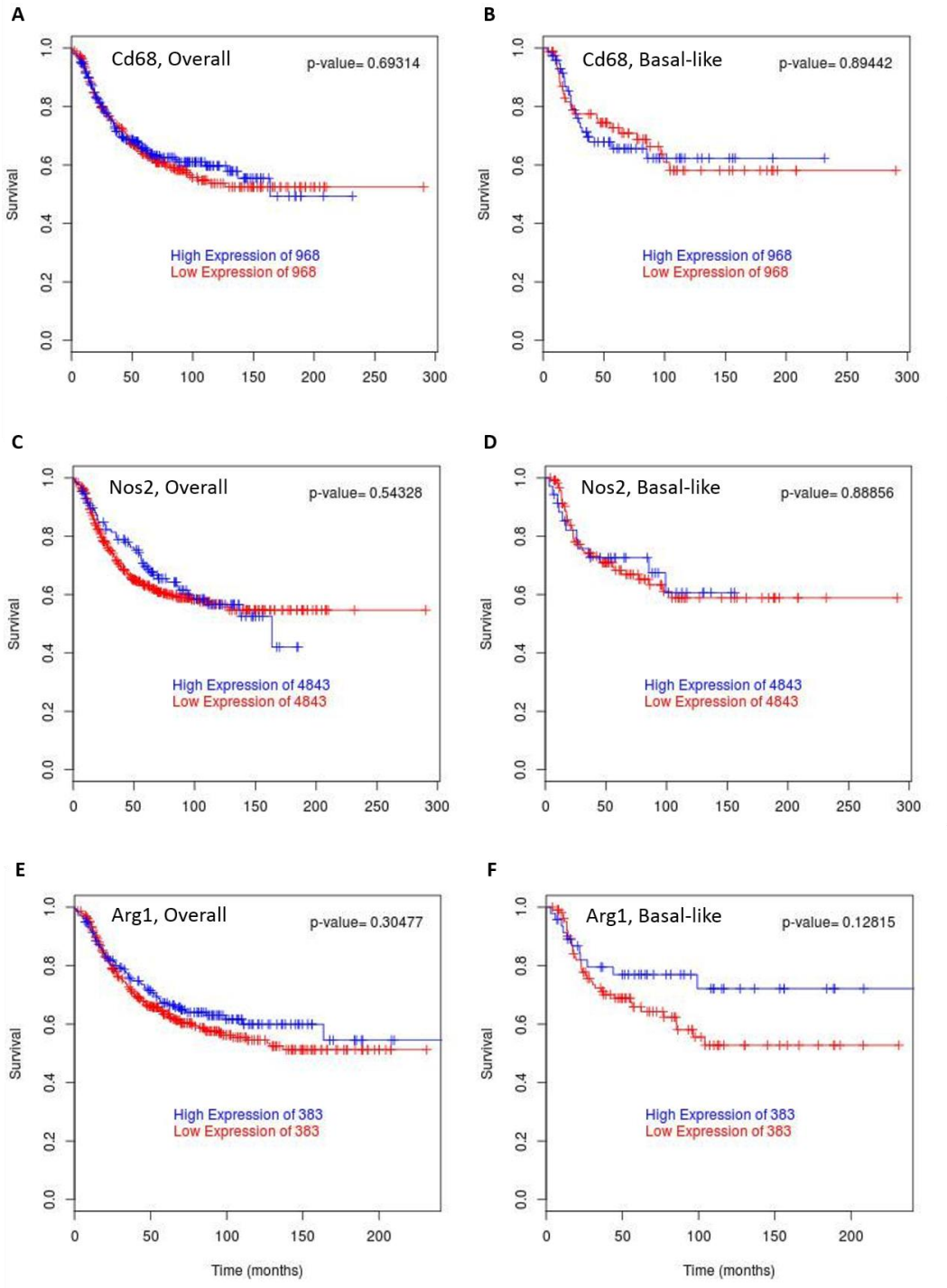

Figure 3.4: Correlation between mRNA expression of Cd68, Nos2 and Arg1 and the survival endpoint of the breast cancer as whole and basal like

In this graph, cut-off is used to dichotomize the data, allowing stratification into high and low groups within each of the individual datasets. The High Expression group in each plot (blue) have expression greater than the cut-off the Low Expression group (red) have expression less than the cut-off, in each of the individual datasets and this is then combined to perform a global pooled survival analysis. N is the number of samples used in this comparison. The Hazard ratio is generated using Cox regression and a log rank test is used to assign significance to the Hazard ratio. The Hazard ratio always relates to increased expression of the marker. **A)** N= 544, Number of events=201, Hazard ration=0.9454 (0.7151 - 1.25). **B)** N= 154, Number of events=49, Hazard ration=1.039 (0.5919 - 1.823). **C)** N= 544, Number of events=201, Hazard ration=0.9044 (0.6537 - 1.251) **D)** N= 154, Number of events=49, Hazard ration=0.9529 (0.4867 - 1.866) **E)** N= 544, Number of events=201, Hazard ration=0.8545 (0.6324 - 1.154). **F)** N= 154, Number of events=49, Hazard ration=0.5965 (0.3044 - 1.169).

3.2.2 Different protein expression level of ARG1 were observed in 66cl4 and 67NR primary tumors and cell line by immunoblotting

Macrophage infiltration within primary tumor environment can correlated with metastatic potential of the tumor. M2 macrophages can increase tumor metastasis (73). Western blot analysis was performed in order to investigate infiltration and polarization of macrophages in metastatic 66cl4 and non-metastatic 67NR primary tumors. Therefore, protein expression of ARG1 and NOS2 in the 66cl4 and 67NR tumors was assessed. RAW264.7 cell stimulated with IFN-γ and LPS was used as control for NOS2 expression. NOS2 expression was not detected in cancer cells and primary tumors. ARG1 expression was detected in 66cl4primary tumor while its expression in 67NR primary tumor and both cancer cell lines could not be observed (Figure3.5). This difference can be assumed as macrophages polarization variant within primary tumors.

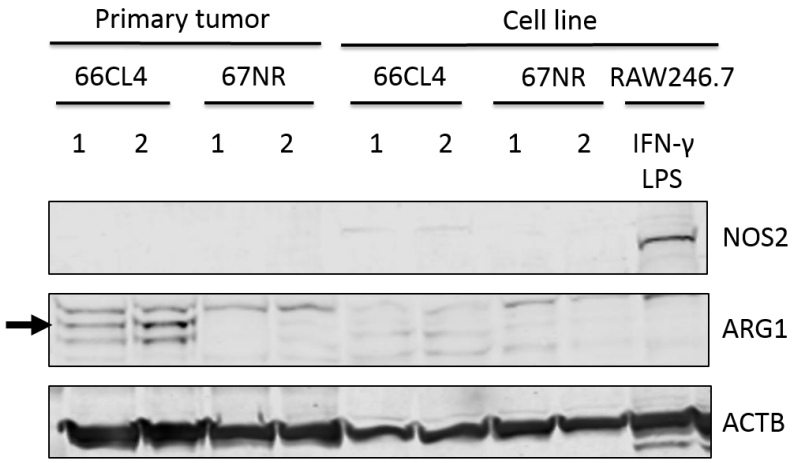

Figure 3.5: Different level of NOS2 and ARG1 were expressed in 66cl4 and 67NR primary tumors and cancer cell lines
Stimulated RAW264.7 cells with IFN-γ and LPS were used as a positive control for NOS2 expression. Membrane was stained for NOS2 (125 kDa), ARG1 (37 kDa) and ACTB (42 kDa) as loading control. Labelled bonds were detected with odyssey near infrared imager. Number above the first band represents different replicate for each sample. Protein expression of ARG1 can be observed in 66cl4 primary tumor lysates (black arrow).

3.2.3 Macrophages could not be localized in 66cl4 primary tumor sections by immunostaining of ARG1 and NOS2

Although H&E staining technique can be used for pathological prognosis, precise identification of specific cells needs a more accurate method. In order to localize and identify polarized macrophages within 66cl4 primary tumor, FFPE 66cl4 tumor sections were stained for ARG1 and NOS2 macrophage markers and scanned with Odyssey infrared imaging system (Figure 3.5). Negative controls were only stained with secondary antibodies (Figure3.5, 2). The same

regions were stained for NOS2 and ARG1 over the section (Figure3.5, 1). Therefore, localizing macrophages was not possible in this assay. Two different conclusions can be resulted. First, primary antibodies were not specific and specialized for this assay. Second, this technique is not sensitive enough distinguishing between macrophage subtypes. Consequently, more sensitive system such as confocal microscopy that can scan sections with higher resolution was needed.

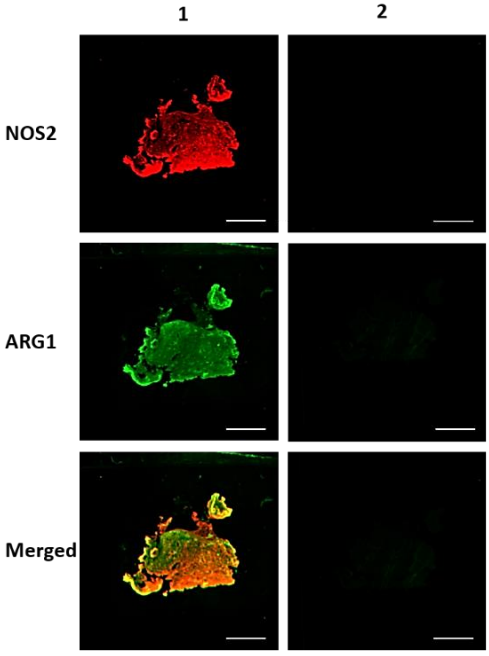

Figure 3.5: Macrophage localization in 66cl4 primary tumor sections using immunostaining by florescent secondary antibodies
1) 66cl4 primary tumor sections were stained using NOS2 and ARG1 primary antibodies and florescent secondary antibodies. **2)** Negative controls were only stained with secondary antibodies.
Sections were scanned using Odyssey infrared imager. No clear difference was observed between stained proteins for NOS2 (red, 680nm) and ARG1 (green, 800nm). Single stained images for NOS2 and ARG1 are shown, together with merged images containing NOS2 and ARG1. The scale bar in the right corner is 1cm (one pixel on the picture is about one cell).

3.2.4 Macrophages could not be localized in 66cl4 and 67NR primary tumor sections utilizing confocal microscopy

In order to localize macrophages within 66cl4 and 67NR primary tumors, FFPE sections were stained for CD68 as general macrophage marker. In order to facilitate discrimination between tumor and non-tumor cells, GFP tagged tumor cells were injected to the BALB/cfC3H mouse. GFP tagged tumor cells would expected to emit green florescent and be easier distinguished from macrophages. Both 66cl4 (Figure3.6, A) and 67NR primary tumor (Figure3.6, B) sections were stained with CD68 primary antibody and secondary antibody that can be detected by confocal microscopy. 66cl4 and 67NR negative controls (slides number 3) that were not stained

with primary antibodies demonstrated nonspecific signal. No clear difference in staining between negative controls and the stained sections was observed. It can be due to autofluorescence of samples, nonspecific binding of secondary antibodies or even fail in tagging tumor cells with GFP.

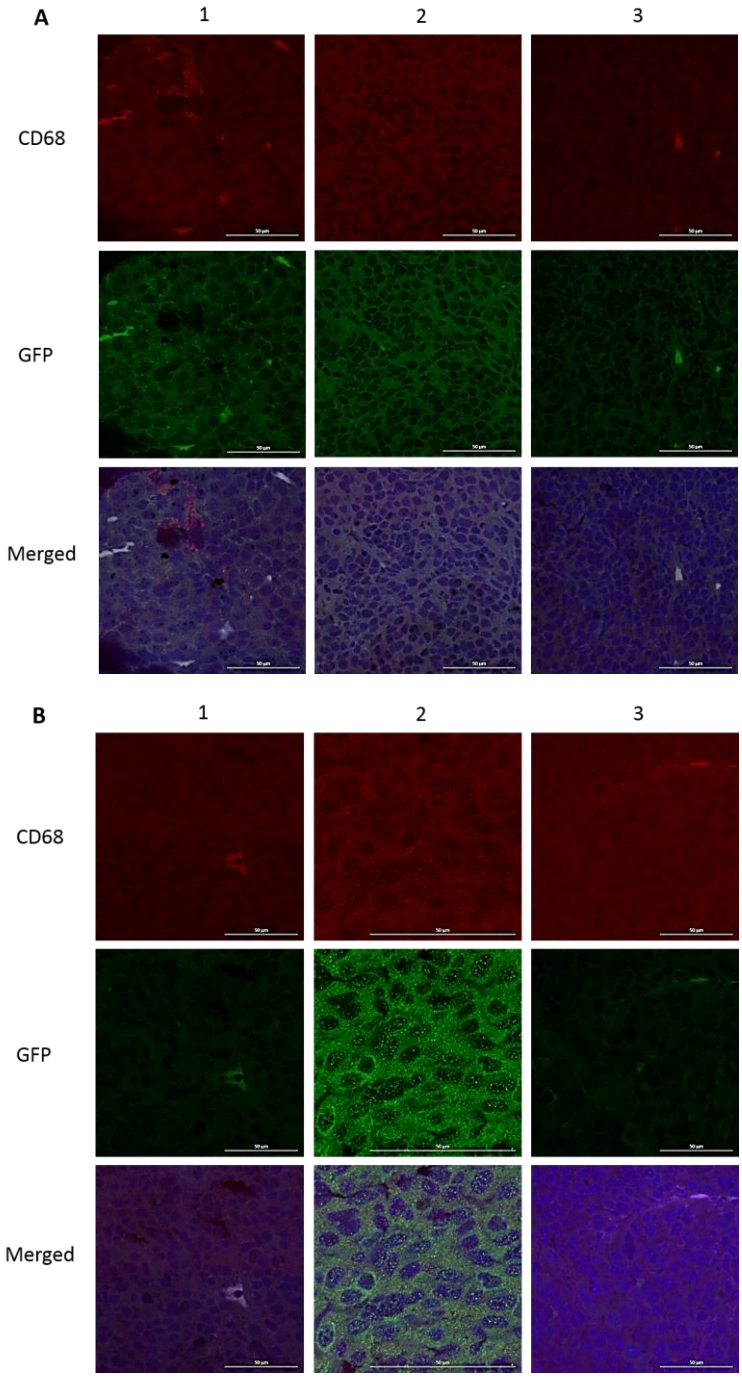

Figure 3.6: Macrophages could not be localized in 66cl4 and 67NR primary tumor sections utilizing confocal microscopy
A) 66cl4 primary tumor sections **B)** 67NR primary tumor sections.
All the sections were stained for CD68 (red), GFP (green) and for nuclei with DRAQ5 dye (blue). Slides 1 and 2 were stained with both primary and secondary antibodies. Sections number 3 were only stained with secondary antibodies (negative control). Secondary antibodies are conjugated with alexa555 (CD68, red) and alexa488 dye (GFP, green). Single stained images for CD68 and GFP are shown, together with merged images containing CD68, GFP and nucleus staining. The bar in the right corner is 50µm.

3.3 RAW264.7 cell line is not suitable for designing an *in vitro* model to study Interaction of 66cl4 and 67NR breast cancer cells and macrophages

Metastasis is the leading cause of death in breast cancer patients. Two mouse cell lines 66cl4 (metastatic) and 67NR (non-metastatic) primary tumors demonstrated different metastatic potential. TAMs are known for contribution in tumor metastasis. Based on previous result explained in section 1 and 2 of the result chapter, it was assumed that macrophages are present in the 66cl4 primary tumors. Complexity of breast tumor microenvironment is a barrier for studying interaction of tumor cells with normal cells. Modeling interaction of macrophages with 66cl4 and 67NR primary tumors can lead to more understanding about tumor progression and the more aggressive growth of 66cl4 tumors. First important step is finding a macrophage cell type that is easy to handle and can change polarization by different stimuli. Different macrophage cell lines can be used for this purpose. RAW264.7 is a mouse-derived cell line; therefore, it can be a good option for studying tumor and macrophage interaction. Chen F *et al*., 2014 considered mouse RAW264.7 macrophage cell line as "M0" that can be polarized toward M1/M2 macrophages by different maturation methods (131). Therefore, polarization of RAW264.7 cells tumor cell co-cultures or after adding conditioned medium from the cancer cells was investigated.

3.3.1 Macrophage polarization cannot be observed by immunostaining RAW264.7 cells treated with conditioned medium of 66cl4 and 67NR

The first step for testing the designed *in vitro* model was to investigate whether culturing RAW264.7 macrophage cells with conditioned medium of 66cl4 and 67NR cells can change the macrophage polarization. RAW264.7 cells reactivity potential to extracellular stimulation, can introduce this cell line as a good option for future research. RAW264.7 cells were seeded in confocal plate in presence of 50% or 100% conditioned medium of 66cl4 and 67NR. Combination of IFN-γ plus LPS and IL4 were used as a positive control for M1 and M2 polarization, respectively. Stimulated cells were stained for NOS2 and ARG1 and analysed by confocal microscopy (Figure3.8). ARG1 positive staining was observed in the negative control, therefore, results are not comparative and trustable. However, comparison between different stimulations implies that more likely conditioned mediums could not effect RAW264.7 cells polarization. It seems that RAW264.7 cells stimulation with IFN-γ and LPS could increase NOS2 expression compared to negative control and other stimulations. However, this result should be confirmed by other methods such as Western blotting.

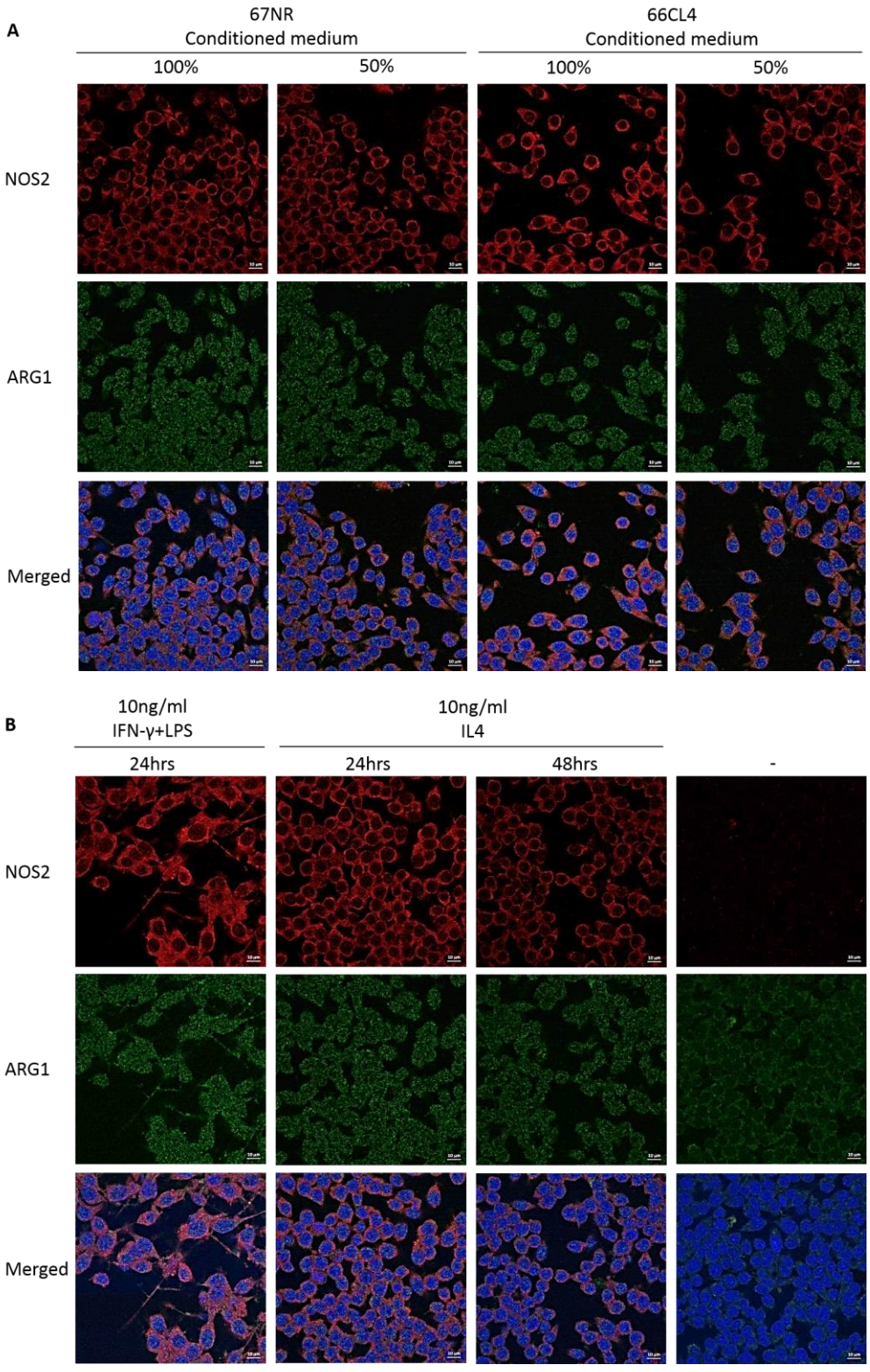

Figure3.8: It is impossible to observe NOS2 and Arg1 protein expression in stimulated RAW 264.7 cells by confocal microscopy

A) RAW264.7 cells were treated with 66cl4 and 67NR conditioned mediums (50% and 100%). **B)** RAW264.7 cells were stimulated using IFN-γ (10ng/ml) and LPS (10ng/ml) or IL4 (10ng/ml). Negative control (-) was not stimulated and only stained with secondary antibodies.

Seeded cells were stained for macrophage markers NOS2 and ARG1 and for nuclei with DRAQ5 dye (blue). Secondary antibodies are conjugated with alexa555 (NOS2, red) and alexa488 dye (ARG1, green). Single stained images for NOS2 and ARG1 are shown, together with merged images containing NOS2, ARG1 and nucleus staining. The bar in the right corner is 10µm.

3.3.2 No difference in proteins expression level of NOS2 and ARG1 in RAW264.7 cells treated with conditioned medium

No confidential difference in RAW264.7 macrophage polarization using conditioned medium of cancer cells was observed by immunostaining. By using western blot, changes in protein expression level of NOS2 and ARG1 as macrophage markers using conditioned medium of cancer cells can be investigated. RAW264.7 cells were seeded in plates and harvested for immunoblotting. Lysate from 66cl4 primary tumor was used as a positive control for ARG1 expression. Unstimulated cells were used as negative control. RAW264.7 cells stimulated with IFN-γ and LPS or IL4 were used as positive control for M1 and M2 polarization, respectively. No difference in morphology of the cells after stimulation using light microscope was observed. Membrane was stained for NOS2 and ARG1 antibodies. Immunoblot analysis demonstrated that RAW264.7 cells are responsive to IFN-γ and LPS stimulation and express NOS2 (Figure3.9). This result can proof results from immunostaining. In addition, RAW264.7 cells did not express ARG1 after stimulation with IL4 with different concentrations and at different time-points.No difference in expression of NOS2 and ARG1 proteins in cells treated by conditioned medium compared to negative control was observed.

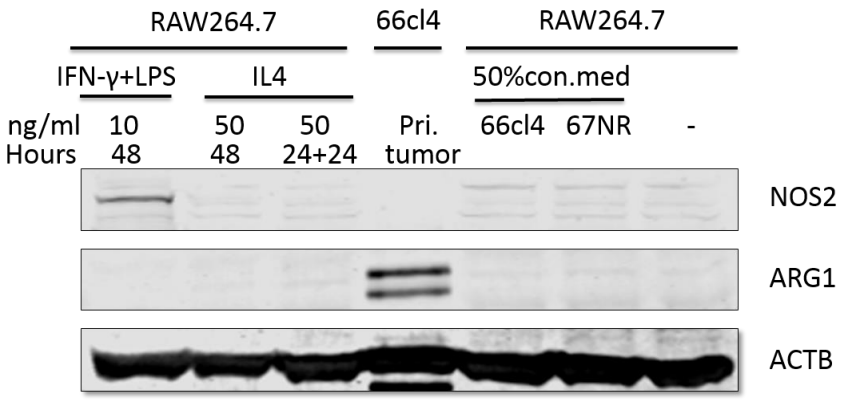

Figure 3.9: No difference in protein expression level of NOS2 and ARG1 was observed in treated RAW264.7 macrophages with conditioned mediums of 66cl4 and 67NR
RAW264.7 macrophage cells were treated with 50% conditioned medium of 66cl4 or 67NR for 48 hours. Positive control cells were stimulated using 10ng/ml IFN-γ and LPS or 50 ng/ml IL4 at different time points (48 hours or 24+24 hours). 66cl4 primary tumor cell lysate was loaded as a positive control of ARG1 protein expression. Un stimulated control is indicated by '-'in the image. Membrane was stained for NOS2 (125 kDa), ARG1 (37 kDa) and ACTB (42 kDa) as loading control.

3.3.3 No mRNA expression of Nos2, Cd163 and Arg1 and no difference in expression of Cd74 was observed in RAW264.7 cells stimulated by conditioned mediums

Western blotting could not detect polarization in RAW264.7 cells by stimulation with conditioned medium of 66cl4 and 67NR. This can be due to the low protein expression level and insensitivity of method for detecting that. Thus, expression of two M1 macrophage markers CD74 and iNOS and two M2 macrophage markers Cd163 and Arg1 was assessed by RT-qPCR. RAW264.7 cell were stimulated with conditioned medium of 66cl4 and 67NR, IFN-γ plus LPS and IL4. In addition, in order to increase cells interaction without direct physical contact, cells were cultured in trans-well. Results from this assay demonstrated no expression of Nos2, Cd163 and Arg1in stimulated samples. Ct values for these genes were so high (more than 30-35 cycle) even by increasing cDNA concentration from 5ng/µl to 50ng/µl; therefore, the data obtained from those genes was not trustable. Nos2, Cd163 and Arg1 mRNAs were not expressed in the samples. Expression of Cd74 could be analyzed due to the lower Ct values (Figure3.10). IFN-γ and LPS stimulation upregulated Cd74 expression in RAW264.7 macrophages. No significant upregulation of Cd74 mRNA expression was observed in RAW264.7 cells using trans-well and condition medium of 66cl4 and 67NR cancer cells (P>o.o5).

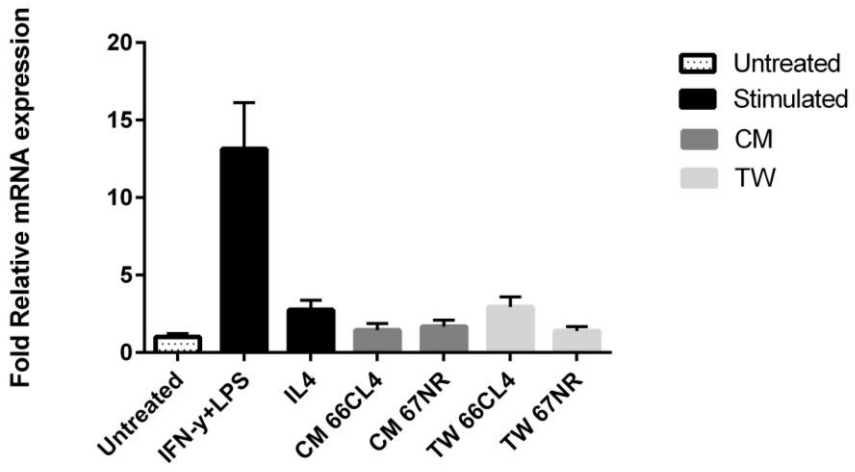

Figure3.10: No significant difference in expression level of Cd74 in stimulated RAW264.7 cells was assayed by quantitative real-time PCR (qPCR)
RAW264.7 cells were stimulated by 50% conditioned medium of 66cl4 and 67NR or co-cultured in a trans-well dish with 66cl4 and 67NR cells. RAW264.7 cells were also stimulated with IFN-γ and LPS 10ng/ml (24hours) or IL4 10ng/ml (24 hours) as positive controls. Fold changes of RNA expression level of Cd74 gene in stimulated samples was compared to untreated using t-test's statistical significance analysis. Standard deviation (SD) is shown in the figure as a bar (n=3).

3.4 IC-21 cell line is not suitable for designing an *in vitro* model in order to study Interaction of 66cl4 and 67NR breast cancer cells and macrophages

As studies in section 3 of the result chapter demonstrated, RAW264.7 macrophages did not respond to stimulation by conditioned medium or co-culture with cancer cells. Therefore, this cell line is not suitable for designing an *in vitro* model for studying macrophage and breast cancer cells interplay. Thus IC-21 cell line was tested for aim of this study. IC-21 is a C57BL/6 mouse adherent cell line was. Consequently, polarization of IC-21 macrophages in presence of different stimuli was assessed.

3.4.1 No difference in protein expression of NOS2 and ARG1 in treated IC-21 cells with conditioned mediums was observed

In order to investigate influence of different stimuli on IC-21 macrophages, these cells were cultured in the presence of 50% 66cl4 and 67NR conditioned mediums. Controls were untreated or stimulated with IFN-γ and LPS or IL4. Cells with different stimulations were monitored using EVOS cell imaging microscope. No significant difference in morphology of IC-21 cells was observed. Immunoblot analysis demonstrated an increase in NOS2 protein level by stimulating IC-21 cells with IFN-γ and LPS (Figure3.11), although to a lesser extent than RAW264.7 cell. In addition, IC-21 cells did not express ARG1 after IL4 stimulation. No difference in expression of NOS2 and ARG1 proteins in cells treated by conditioned medium was observed.

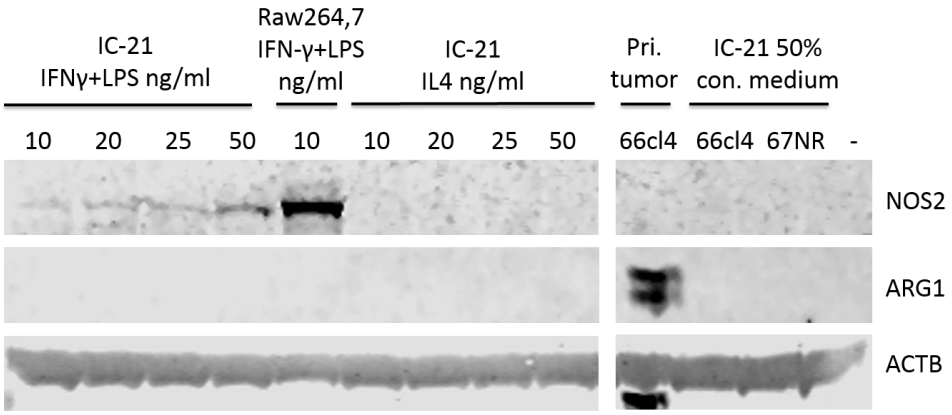

Figure 3.11: No difference in protein expression of NOS2 and ARG1 in treated IC-21 cells with conditioned mediums was observed
Seeded IC-21 cells were stimulated for 48hours using 50% conditioned medium of 66cl4 or 67NR. Controls were stimulated using 10, 20, 25 and 50ng/ml IFN-γ and LPS or 10, 20, 25 and 50 ng/ml IL4 for 24 hours. 66cl4 primary tumor cell lysate was loaded as a positive control of ARG1 protein expression. Unstimulated control was indicated by '-'in the image. Membrane was stained for NOS2 (125 kDa), ARG1 (37 kDa) and ACTB (42 kDa) as loading control.

4. Discussion

The two breast cancer cell lines 66cl4 and 67NR have different metastatic potential (118, 119). Tumor microenvironment constitution can influence tumors characteristics (21). Genotyping results demonstrated that about 40% of 66cl4 and 30% of 67NR primary tumors consist of non-tumor cells. Macrophages are important compartments of tumor microenvironment that contribute in breast carcinogenesis (96-98). TAMs associating tumor progression are predominantly M2 macrophages (132). Based on immune blot and transcriptome data analysis, it can be assumed that more M2 macrophages infiltrated within 66cl4 primary tumor than 67NR. Metastasis and cancer progression is a complex phenomenon that can be depended on different stroma cell types. Therefore, it would be more practical to study interaction of tumor cells and macrophages *in vitro*. Two different macrophage cell lines were chosen for designing this model. Experimental data suggests that RAW264.7 and IC-21 macrophage cell lines are not ideal models for studying this interaction.

4.1 66cl4 and 67NR primary tumors heterogeneity is due to infiltrated cells

Tumor microenvironment contributes to tumor suppression or growth and metastasis(22). It is well evident that breast cancer cells continuously interact with infiltrated non-tumor cells including immune cells in the tumor microenvironment (133). It is notable that each tumors is unique regarding to their microenvironment (22). It is interesting to compare metastatic and non-metastatic tumors heterogeneity, cellular composition and different infiltrated cellular polarization. This information can help understanding correlation between infiltrated cells with metastasis. A wide range of experimental models can be used for studying different aspects of breast tumor carcinogenesis (112). However, based on aim of this study, it is valuable to investigate tumor cellular composition in a syngeneic, non-manipulated mouse model with a functioning immune system.

Tumor cell composition can be characterized and distinguished by investigating specific cell markers expression. A number of reports suggest a variety of markers for different cell type. Comparing expression of these markers with the transcriptome data can help choosing the most suitable marker for the study. Analyzing transcriptome data of cultured cells and primary tumor of 66cl4 and 67NR represents valuable information regarding sum of the cells in the primary tumors. Low mRNA expression in the breast cancer cells and higher expression in primary tumors can indicate possible infiltration of different immune cells within the primary tumors.

Based on transcriptome data analysis, three different macrophage markers were chosen for further investigation. CD68, ARG1 and NOS2 are general, M2 and M1 macrophage markers, respectively (134). Transcriptome data analysis demonstrated higher mRNA expression of Cd68 and Nos2 in primary tumors than breast cancer cells. Low Arg1 mRNA expression in both breast cancer cells and 67NR primary tumor than 66cl4 primary tumor might be due to the higher infiltration of M2 macrophages in 66cl4 primary tumor than 67NR. In addition, same trend was observed in other macrophage marker candidates. It is notable that there might be other macrophage markers in the transcriptome data that can be analyzed for more precise calculation.

Based on average expression of macrophage markers, it can be interpreted that macrophages are infiltrated to 66cl4 and 67NR primary tumors. However, it should be noted that upregulation of genes in primary tumors compared to cancer cells, does not necessarily correlate with cell infiltration. All of these markers can be upregulated in primary tumors and also be expressed by other cell types than what it is mentioned in some literature. For example CD68 has been known as a macrophage marker (47, 134). Kunz-Schughart LA *et al*., 2003 investigated CD68 protein and gene expression in fibroblasts. They have claimed that CD68 is not only expressed in macrophage lineage but also fibroblasts isolated from normal and tumor breast tissue express CD68 at comparable level to macrophages (135). Therefore, further investigation regarding macrophage infiltration is necessary.

It is notable that analysis of transcriptome data can give hints of type infiltrated cells but not number of cells since both increased number of cells and increased expression of a marker in few cells can influence mRNA expression level.

For estimating number of infiltrated cells to the tumor microenvironment, SNP frequency was analyzed. This primer assay was designed based on identification of a homozygous point mutation in both 66cl4 and 67NR cancer cell lines that does not exist in BALB/cfC3H mouse. This novel approach tried to estimate percentage of non-tumor cells within 66cl4 and 67NR primary tumor by investigating frequency of mutated allele (A/A) and wild-type allele (G/G) in the tumor samples. Sequence detection system in the Real-Time PCR system had measured florescence signal before and after the amplification. Relative quantification of allele's ΔRn was done in order to assess relative amount of the target nucleic acid in samples by comparing each samples with calibrator. Here calibrator for mutated allele is 66cl4 and for wild-type allele is RAW264.7 or BALB/cfC3H blood. For first test, in order to test accuracy and sensitivity of this method and designed primers standard curve was plotted. Result from allele 1 demonstrated a linear decrease in number of tumor cells by reducing percentage of 66cl4 DNA. In contrary,

results from allele 2 is not comparative with volume of pipetted DNA. PCR conditions might not be optimal and can lead to these deviations. Errors in probe designing cam cause this deviation as well. However, results suggested that allele 1 might be suitable for calculating percentage of nun-tumor cells within primary tumor samples.

This statistical analysis was based on mathematical approaches and relative quantification that is common technique for RT-qPCR. Assessing results from this experiment suggests that sample ΔRn can be used for estimating percentage of tumor and non-tumor cells within a primary tumor.

In order to estimate number of tumor and non-tumor cells within a primary tumor of 66cl4 and 67NR, allele frequency was determined using TaqMan SNP genotyping assay. Statistical analysis demonstrated that almost 40% of 66cl4 primary tumors and 30% of 67NR primary tumors are consist of non-tumor cells. Comparing these results with results from transcriptome data analysis demonstrated infiltration of cells within primary tumors of 66cl4. Previous studies have also demonstrated infiltration of immune cells such as lymphocytes (136) and macrophages (137) to breast tumor. Infiltrated immune cells play an important role in cancer related inflammation (33) and macrophages represent a major component of infiltrated cells within solid tumors (138).

This assay can be limited by technical error. Tumor isolation can be along with isolation of the tissue that surrounded the tumor that can influence the results and increase number of non-tumor cells in the sample. However, in order to increase accuracy of the study, several samples of 66cl4 and 67NR primary tumors were analyzed. Producer suggested post-plate read (139). In this experiment sample ΔRn was obtained by pre and post plate read. Plate reading during amplification can indicate Ct values that are used in RT-qPCR relative calculations (122). For future study, Ct value can be substituted with ΔRn for allele frequency calculation. In addition, accuracy of this technique can be examined by plotting standard curve for 67NR. BALB/cfC3H mouse blood can be used instead of RAW264.7 cells in order to increase precision of the experiment and for data comparison.

This assay demonstrated valuable information regarding percentage of tumor and non-tumor cells within 66cl4 and 67NR primary tumors. However, these results do not provide any information about non-tumor cellular composition and its contribution in the primary tumors suppression or progression. Characterizing different cell types in the primary tumor allow a more precise interpretation of their function in breast tumor.

In order to identify infiltrated cells within primary tumors of 66cl4 and 67NR, H&E stained sections were assessed. Analysis H&E stained sections demonstrated heterogeneity in 66cl4

primary tumor sections. In 67NR primary tumor sections, tumor cells were in close distance to each other and cells were seem similar. Results from genotyping assay suggested heterogeneity in both 66cl4 and 67NR primary tumors, however in 67NR primary tumor unique section pattern was observed. This result is contradictory with genotyping and transcriptome data results that suggest non-tumor cell infiltration within both primary tumors. H&E staining is not the best option for studying tissue cellular compartment but it is an initiation for further staining. Other techniques such as immunofluorescence staining allows us to stain for different cell type and distinguish easier without need to know morphology of each cell. Thus, markers that have been chosen based on literature and transcriptome data can possibly stain for protein of interest (CD68, ARG1 and NOS2) by other techniques such as immunofluorescence staining.

4.2 66cl4 and 67NR tumor heterogeneity is due to the presence of polarized macrophages, M2 macrophages in particular

Macrophage can constitute up to 80% of leukocyte in final stage of mouse mammary carcinoma (31). Previous studies demonstrated role of infiltrated TAMs in breast tumor progression (96-98). Macrophages can be schematically sub divided to M1 and M2 macrophages (41, 52). M1 macrophage are important players of the innate immune defense (54) while M2 macrophages increase tumor metastasis and immune suppression in tumor microenvironment (73). TAMs associating tumor progression are predominantly M2 macrophages (132).

Based on literature study and results from the first part of the project, this study focused on macrophage polarization in 66cl4 and 67NR primary tumors. Aim of all animal models is to mimic human disease conditions. In order to investigate relation between patient survival rate and CD68, ARG1 and NOS2 macrophage markers gene expression Breast Mark online database was investigated. According to this database, there is no correlation between survival rate in breast cancer patient and expression of Cd68, Arg1and Nos2 genes. However, studies described function of TAMs in breast carcinogenesis (96-98). It has been claimed that higher number of TAMs do not always correlate with worse prognosis. However, different macrophage localization can correlate with patient survival (140).

Brian Ruffell *et al.*, 2012 expressed that CD68 is not a specific macrophage marker for human breast cancer (31). Therefore, there might be other macrophage markers that are more specific and upregulated in human breast cancer that also correlates with patient survival. Thus, this result does not deny the role of macrophages in breast tumor carcinogenesis. Assessing transcriptome data in this mouse model demonstrated differences in mRNA expression of these

macrophage markers in mouse breast cancer cells and primary tumors. Therefore, it was assumed that these markers could be used for localizing and characterizing infiltrated macrophages in this study. Generally, in order to increase accuracy of future human and mouse studies, more than one macrophage marker can be investigated.

In contrary, there are studies that claimed expression of CD68 in tumor stroma correlates with reduced overall breast cancer survival (47, 81). It would be beneficial to investigate breast cancer as a whole, as its survival can depend on parallel factors. As it has been established, $CD68^+$ cell density alone showed no statistical significance in overall survival. However, low $CD8^+$ T_c and high $CD68^+$ correlates with reduced overall survival in basal like breast cancer (95). It is noticeable that results from these studies and breast mark is influenced by number of patients as well.

Western blot analysis was performed in order to investigate macrophage infiltration within primary tumors. Therefore, protein expression of ARG1 and NOS2 in the 66cl4 and 67NR primary tumor was investigated. Expression of ARG1 in aggressive 66cl4primary tumor was detected while its expression in 67NR primary tumor and both cancer cell lines could not be observed. As it can be seen in the immune blot, expression of NOS2 was not detected in primary tumors. Transcriptome data analysis results correlates with the detection of NOS2 and ARG1 in western blots of the tumor extracts. Based on transcriptome data, Arg1 is expressed higher in 66cl4 than 67NR primary tumor and Nos2 is low expressed in both primary tumors. It is notable that mRNA level does not necessarily correlates with protein levels. Movahedi *et al*., 2010 have also stated higher arginase activity in TAMs in the mouse breast cancer model (132). This difference can be assumed as macrophages phenotypic variance within different primary tumors. Based on immune blot and transcriptome data analysis, it can be assumed that M2 macrophages are higher infiltrated in 66cl4 primary tumors than 67NR. However, it needs more experimental support since expression of macrophage marker proteins could be too low to be detected in 67NR primary tumor by this technique. However, in order to compare protein expression of M1 macrophage markers within primary tumors, other markers such as CD74 can be chosen for future studies.

As it has been mentioned, higher number of TAMs do not always correlate with worse prognosis. However, different macrophage localization can correlate with patient survival (140). Plethora of macrophages can be seen at margin of the mouse mammary tumors (141) and macrophages present in hypoxic area are more M2-like (142). Therefore, macrophage localization using immunofluorescence staining can lead to better comprehension of its function within breast tumor and can facilitate macrophage cognition. FFPE 66cl4 tumor sections were

stained for ARG1 and NOS2 antibodies and scanned with Odyssey scanner. Resolution of odyssey scanner is not high and does not enable distinguishing between cells (one pixel on a picture is about one cell). The same regions were stained for NOS2 and ARG1 over the sections and macrophages identification by immunofluorescence staining was not possible. Based on genotyping results, almost 60% of 66cl4 primary tumors constitute of tumor cells. Therefore, it was expected that some parts of the sections were not stained with macrophage markers. Nonspecific binding of primary antibodies and technical problems in sections preparation can cause errors in staining.

As the previous staining technique was not specific for macrophage localization using odyssey scanner was not possible. Therefore, 66cl4 and 67NR primary tumor sections were stained for CD68 primary and fluorescent secondary antibodies. For this experiment, GFP tagged tumor cells were injected to the BALB/cfC3H mouse to facilitate discrimination between tumor and non-tumor cells. Thus, tumor cells would be detected with green florescent. No clear difference in staining between negative controls and the stained sections was observed.

Working with confocal microscope needs practice and there are several technical details regarding microscope set up that can influence quality and resolution of the images. For instance, high gain value can generate pseudo-florescence signal and create false positive result. Fixation mistakes can cause cell dryness that would be seen as artifacts in the section.

Due to the macrophages heterogeneity, even more than one marker cannot necessarily detect all the population (143). Thus, for future studies more than one macrophage markers should be chosen. Macrophages are distributed in normal liver and spleen (143); therefore, these tissues can be used as a positive control for future staining. However, this study was planned by the tissues and material that were accessible.

4.3 RAW264.7 and IC-21 cells are not suitable *in vitro* models for studying interaction of 66cl4 breast cancer cells and macrophages

Models giving chance of simplifying *in vivo* interactions, mimic *in vivo* environment in a co-culture, and manipulate conditions. Interaction of tumor cells with its microenvironment can effect tumor growth and metastasis (21). Based on results of this study, it was assumed that macrophages are present in the 66cl4 primary tumors. An *in vitro* model enables studying interaction of tumor cells and macrophages in a simplified defined condition. Different cells can be used for this study; bone marrow-derived macrophages (BMDM), peritoneal macrophages and also Raw264.7 and IC21 cell lines.

RAW264.7 macrophages is a mouse-derived cell line that does not need any maturation procedure like BMDM. In addition, RAW264.7 macrophage cell line can be assumed as "M0" and be polarized toward M1/M2 subtypes by different cytokines (131). Different polarization of RAW264.7 macrophages in the presence of the cancer cells or conditioned medium of tumor cells was investigated. Macrophages can be polarized to M1 in presence of IFN-γ plus LPS and to M2 macrophages in presence of IL4 (45). M1 maturation upregulate NOS2 and M2 maturation enhance ARG1 expression (144).

Studying interaction of RAW264.7 macrophages with 66cl4 primary tumors can lead to more understanding about aggressive growth of 66cl4 tumors and effect of released cytokines from breast cancer cells on macrophage polarization. Cultured cells that were treated with conditioned mediums of tumor cells were stained for ARG1 and NOS2 and were analyzed using confocal microscope. ARG1 positive staining was observed in the negative control, therefore, results are not comparative and trustable. A slight difference in RAW264.7 cells stimulated with IFN-γ and LPS was observed. Obtained results implies that more likely conditioned mediums could not effect RAW264.7 cells polarization.

Immune blot analysis was performed in order to observe protein expression of NOS2 and ARG1 on stimulated RAW264.7 with conditioned medium of 66cl4 and 67NR. Immune blot analysis demonstrated no expression in macrophage markers after stimulation with conditioned medium of 66cl4 and 67NR. However, RAW264.7 macrophages expressed NOS2 after stimulation with IFN-γ and LPS and the same trend was observed in immunofluorescence stained cells.

Negative IL4 stimulation could not be due to un-bioactive recombinant cytokines because bio reactivity of cytokines was previously tested on BMDM by other member of the group. It is probable that expression of Nos2 and Arg1 genes are not high so it is hard to observe protein expressions on a blotted membrane. Therefore, mRNA expression of Cd74 and Nos2 as M1 macrophage markers and ARG1 and Cd163 as M2 macrophage markers in co-cultures and stimulated cells with conditioned medium of 66cl4 and 67NR was investigated. For this step of study, cells were co-cultured in trans-wells in order to increase interaction of cells and probably observe changes in macrophage polarization *in vitro*.

Expression of Cd74 was analysed due to the low Ct value. Statistical analysis demonstrated upregulation of Cd74 after stimulation with IFN-γ and LPS. Results from florescent stained cells and immune blot demonstrated M1 macrophage polarization after IFN-γ plus LPS stimulation. However, no significant up regulation of Cd74 mRNA expression in trans-wells and stimulated cells with conditioned mediums was observed.

Results from RT-qPCR assay demonstrated no mRNA expression of Nos2, Cd163 and Arg1 in samples. High Ct values can demonstrate absence of Nos2, Cd163 and Arg1 mRNA in cells.
Results from mRNA expression level of Arg1 demonstrate nonspecific staining results from stained RAW264.7 cells stimulated with IL4 since ARG1 was expressed in all samples. Those results can be due to auto-florescence of the cells because when gene is not expressed, protein expression cannot be high. Gao S et at., 2014 demonstrated that Arg1 mRNA expression has increased after 12 hours stimulation with IL4 (10ng/ml) compared to unstimulated (145). Therefore, protocol can be improved by using more stimulation time points for further analysis. It can be assumed that these genes are not expressed in RAW264.7 cells stimulated with conditioned medium of 66cl4 and 67NR cancer cells or this technique is not sensitive enough for measuring mRNA expression in this assay.
RAW264.7 macrophage cells have been used for designing a model for studying interaction of rat breast cancer cells with macrophages (146). However, based on the results of this study, it was concluded that RAW264.7 cell line is not suitable for modeling interaction of macrophages with 66cl4 breast cancer cells. Therefore, IC-21 macrophages were chosen to study interaction of macrophages with cancer cells. IC-21 is a C57BL/6 mouse adherent cell line that has been used for inflammatory models (147). IC-21 mouse macrophage cells were cultured with conditioned medium of breast cancer cell. No polarization toward M1 or M2 macrophages by immunoblot analysis using conditioned medium of 66cl4 and 67NR cancer cells was detected. Comparing IC-21 cells stimulation status with RAW264.7 macrophages demonstrated that IC-21 cells were less reactive to stimuli. Based on these results IC-21 cell line is not suitable for further investigation.
RAW264.7 and IC-21 cells used for these analysis was obtained from CEMIR group and were with an unknown passage number. Therefore, unresponsive of RAW264.7 and IC-21 cells to stimulation can be due to the high passage number of these cells.
It is notable that both the transformed cell lines RAW264.7 and IC-21 may have partially changed their signaling pathways during development. Therefore, these cell lines are less suitable for studying normal cells regulation.
Parallel experimental analysis by other member of Bjørkøy group demonstrated that BMDM and peritoneal macrophages could be used for studying macrophage and breast cancer cells interaction. BMDM and peritoneal macrophages were polarization toward M1 or M2 by different stimuli and conditioned medium of 66cl4 and 67NR. Therefore, RAW264.7 and IC-21 cell lines will not be used for further experiments.

Results from this study demonstrated that primary tumors stablished by two breast cancer cell lines 66cl4 and 67NR are heterogeneous and non-tumor cells can be polarized into these two primary tumors. The transcriptome data and immunoblot analysis suggests that more M2 macrophages infiltrated within 66cl4 primary tumor than 67NR. Further aim was to investigate interaction of 66cl4 cancer cells and macrophages in an *in vitro* model by using RAW264.7 and IC-21 macrophage cell lines. Results obtained from his study does not recommend this two cell lines for future work.

5. Conclusion and future work

Primary tumors established by two breast cancer cell lines 66cl4 and 67NR have different metastatic potential and represent a good model to study mechanisms that might underlay metastasis. Analyzing transcriptome data of cultured cells and primary tumors of 66cl4 and 67NR gives valuable information regarding the sum of the cells in the primary tumors. Absence of mRNA expression of specific markers in the cell culture and higher expression in primary tumors can indicate possible infiltration of the host cells to the primary tumors. Genotyping of primary tumors can be used to estimate the number of non-tumor cells within primary tumors. As it has been calculated, about 40% of 66cl4 and 30% of 67NR primary tumors consist of non-tumor cells that could account for the expression of markers in the tumor that were absent in the cell culture.

Results of this study indicate more heterogeneity in 66cl4 than 67NR primary tumors. Based on transcriptome data and immune blot analysis of ARG1, it can be assumed that M2 macrophages are higher infiltrated within 66cl4 primary tumor than 67NR. However, it has to be verified that ARG1 is not expressed by other cells of the tumors. Overall results demonstrated that M1 marker NOS2 is not detectable in tumor samples.

To study tumor cell-macrophage interactions in the complex tumor microenvironment in more detail, it would be beneficial to establish an *in vitro* model with only two cell types. Culturing 66cl4 and 67NR breast cancer cells with RAW264.7 macrophage cell line did not demonstrate any changes in polarization of the macrophages. In addition, no effect on RAW264.7 and IC-21 cells after treatment of with conditioned medium of both cancer cells was observed. These results suggests that these two macrophage cell lines cannot be ideal models for studying this interaction.

Based on results from Bjørkøy group, BMDM and peritoneal macrophages can be used for *in vitro* modeling of tumor stroma interaction. Future experiments should be focused on compounds secreted by 66cl4 tumor cells that contribute in macrophage recruitment and polarization. Therefore, conditioned medium of 66cl4 and 67NR cancer cells can be analyzed for different cytokines and chemokines by ELISA. Knocking out of these components in 66cl4 tumor cells and studying their interaction with macrophages can also indicate the function of these components in tumor metastasis. Transcriptome data analysis can help choosing suitable targets and confirming results.

Further research should be aimed at investigating other M1 macrophage markers than NOS2 by literature study and transcriptome data analysis. For further studies, better methods to visualize macrophages in primary tumors should be established. RNA *in situ* hybridization (ISH) RNA scope in particular, is a suitable technique that can be used for more accurate targeting different macrophage markers within primary tumors.

References

1. Druesne-Pecollo N, Touvier M, Barrandon E, Chan DS, Norat T, Zelek L, et al. Excess body weight and second primary cancer risk after breast cancer: a systematic review and meta-analysis of prospective studies. Breast cancer research and treatment. 2012;135(3):647-54.
2. DeSantis C, Ma J, Bryan L, Jemal A. Breast cancer statistics, 2013. CA: a cancer journal for clinicians. 2014;64(1):52-62.
3. Cancer IAfRo. Latest world cancer statistics
Global cancer burden rises to 14.1 million new cases in 2012:Marked increase in breast cancers must be addressed 2013.
4. Norway CRo. Cancer in Norway 2012 - Cancer incidence, mortality, survival and prevalence in Norway. 2014.
5. Verma R, Bowen RL, Slater SE, Mihaimeed F, Jones JL. Pathological and epidemiological factors associated with advanced stage at diagnosis of breast cancer. British medical bulletin. 2012;103(1):129-45.
6. Hanahan D, Weinberg RA. The Hallmarks of Cancer. Cell. 2000;100(1):57-70.
7. Hanahan D, Weinberg Robert A. Hallmarks of Cancer: The Next Generation. Cell. 2011;144(5):646-74.
8. Mathew R, Karantza-Wadsworth V, White E. Role of autophagy in cancer. Nat Rev Cancer. 2007;7(12):961-7.
9. Berger AH, Knudson AG, Pandolfi PP. A continuum model for tumour suppression. Nature. 2011;476(7359):163-9.
10. Fearon ER, Vogelstein B. A genetic model for colorectal tumorigenesis. Cell. 1990;61(5):759-67.
11. Alphonso A, Alahari SK. Stromal cells and integrins: conforming to the needs of the tumor microenvironment. Neoplasia (New York, NY). 2009;11(12):1264-71.
12. Viale G. The current state of breast cancer classification. Ann Oncol. 2012;23 Suppl 10:x207-10.
13. Schnitt SJ. Classification and prognosis of invasive breast cancer: from morphology to molecular taxonomy. Mod Pathol. 2010;23(S2):S60-S4.
14. Polyak K. Heterogeneity in breast cancer. The Journal of clinical investigation. 2011;121(10):3786-8.
15. Meric-Bernstam F, Mills GB. Overcoming implementation challenges of personalized cancer therapy. Nature reviews Clinical oncology. 2012;9(9):542-8.
16. Chaffer CL, Weinberg RA. A perspective on cancer cell metastasis. Science (New York, NY). 2011;331(6024):1559-64.
17. Scully OJ, Bay BH, Yip G, Yu Y. Breast cancer metastasis. Cancer genomics & proteomics. 2012;9(5):311-20.
18. Li DM, Feng YM. Signaling mechanism of cell adhesion molecules in breast cancer metastasis: potential therapeutic targets. Breast cancer research and treatment. 2011;128(1):7-21.
19. Joyce JA, Pollard JW. Microenvironmental regulation of metastasis. Nat Rev Cancer. 2009;9(4):239-52.
20. Smith HA, Kang Y. The metastasis-promoting roles of tumor-associated immune cells. Journal of molecular medicine (Berlin, Germany). 2013;91(4):411-29.
21. Quail DF, Joyce JA. Microenvironmental regulation of tumor progression and metastasis. Nat Med. 2013;19(11):1423-37.
22. Ogino S, Fuchs CS, Giovannucci E. How many molecular subtypes? Implications of the unique tumor principle in personalized medicine. Expert review of molecular diagnostics. 2012;12(6):621-8.
23. Ogino S, Galon J, Fuchs CS, Dranoff G. Cancer immunology--analysis of host and tumor factors for personalized medicine. Nature reviews Clinical oncology. 2011;8(12):711-9.

24. Kitamura T, Qian B-Z, Pollard JW. Immune cell promotion of metastasis. Nat Rev Immunol. 2015;15(2):73-86.
25. Mao Y, Keller ET, Garfield DH, Shen K, Wang J. Stromal cells in tumor microenvironment and breast cancer. Cancer metastasis reviews. 2013;32(1-2):303-15.
26. Nieman KM, Kenny HA, Penicka CV, Ladanyi A, Buell-Gutbrod R, Zillhardt MR, et al. Adipocytes promote ovarian cancer metastasis and provide energy for rapid tumor growth. Nat Med. 2011;17(11):1498-503.
27. Delgado VM, Nugnes LG, Colombo LL, Troncoso MF, Fernandez MM, Malchiodi EL, et al. Modulation of endothelial cell migration and angiogenesis: a novel function for the "tandem-repeat" lectin galectin-8. FASEB journal : official publication of the Federation of American Societies for Experimental Biology. 2011;25(1):242-54.
28. Hugo HJ, Lebret S, Tomaskovic-Crook E, Ahmed N, Blick T, Newgreen DF, et al. Contribution of Fibroblast and Mast Cell (Afferent) and Tumor (Efferent) IL-6 Effects within the Tumor Microenvironment. Cancer microenvironment : official journal of the International Cancer Microenvironment Society. 2012.
29. Ostrand-Rosenberg S. Immune surveillance: a balance between protumor and antitumor immunity. Current opinion in genetics & development. 2008;18(1):11-8.
30. Mantovani A. Macrophages, Neutrophils, and Cancer: A Double Edged Sword. New Journal of Science. 2014;2014:14.
31. Ruffell B, Au A, Rugo HS, Esserman LJ, Hwang ES, Coussens LM. Leukocyte composition of human breast cancer. Proceedings of the National Academy of Sciences of the United States of America. 2012;109(8):2796-801.
32. Wesolowski R, Markowitz J, Carson WE, 3rd. Myeloid derived suppressor cells - a new therapeutic target in the treatment of cancer. Journal for immunotherapy of cancer. 2013;1:10.
33. Balkwill F, Mantovani A. Inflammation and cancer: back to Virchow? Lancet. 2001;357(9255):539-45.
34. Ling J, Kumar R. Crosstalk between NFkB and glucocorticoid signaling: a potential target of breast cancer therapy. Cancer letters. 2012;322(2):119-26.
35. Dvorak HF. Tumors: wounds that do not heal. Similarities between tumor stroma generation and wound healing. The New England journal of medicine. 1986;315(26):1650-9.
36. Iyengar NM, Hudis CA, Dannenberg AJ. Obesity and inflammation: new insights into breast cancer development and progression. American Society of Clinical Oncology educational book / ASCO American Society of Clinical Oncology Meeting. 2013:46-51.
37. de Visser KE, Korets LV, Coussens LM. De novo carcinogenesis promoted by chronic inflammation is B lymphocyte dependent. Cancer Cell. 2005;7(5):411-23.
38. Mantovani A, Ming WJ, Balotta C, Abdeljalil B, Bottazzi B. Origin and regulation of tumor-associated macrophages: the role of tumor-derived chemotactic factor. Biochimica et biophysica acta. 1986;865(1):59-67.
39. Murray PJ, Wynn TA. Protective and pathogenic functions of macrophage subsets. Nat Rev Immunol. 2011;11(11):723-37.
40. van Furth R, Cohn ZA. The origin and kinetics of mononuclear phagocytes. The Journal of experimental medicine. 1968;128(3):415-35.
41. Vogel DY, Glim JE, Stavenuiter AW, Breur M, Heijnen P, Amor S, et al. Human macrophage polarization in vitro: maturation and activation methods compared. Immunobiology. 2014;219(9):695-703.
42. Mantovani B, Rabinovitch M, Nussenzweig V. Phagocytosis of immune complexes by macrophages. Different roles of the macrophage receptor sites for complement (C3) and for immunoglobulin (IgG). The Journal of experimental medicine. 1972;135(4):780-92.
43. Buechler C, Ritter M, Orso E, Langmann T, Klucken J, Schmitz G. Regulation of scavenger receptor CD163 expression in human monocytes and macrophages by pro- and antiinflammatory stimuli. Journal of leukocyte biology. 2000;67(1):97-103.

44. Goldstein JL, Ho YK, Basu SK, Brown MS. Binding site on macrophages that mediates uptake and degradation of acetylated low density lipoprotein, producing massive cholesterol deposition. Proceedings of the National Academy of Sciences of the United States of America. 1979;76(1):333-7.
45. Mantovani A, Sozzani S, Locati M, Allavena P, Sica A. Macrophage polarization: tumor-associated macrophages as a paradigm for polarized M2 mononuclear phagocytes. Trends Immunol. 2002;23(11):549-55.
46. Shi C, Pamer EG. Monocyte recruitment during infection and inflammation. Nat Rev Immunol. 2011;11(11):762-74.
47. Medrek C, Ponten F, Jirstrom K, Leandersson K. The presence of tumor associated macrophages in tumor stroma as a prognostic marker for breast cancer patients. BMC cancer. 2012;12:306.
48. Stein M, Keshav S, Harris N, Gordon S. Interleukin 4 potently enhances murine macrophage mannose receptor activity: a marker of alternative immunologic macrophage activation. The Journal of experimental medicine. 1992;176(1):287-92.
49. Waldo SW, Li Y, Buono C, Zhao B, Billings EM, Chang J, et al. Heterogeneity of human macrophages in culture and in atherosclerotic plaques. The American journal of pathology. 2008;172(4):1112-26.
50. Munder M, Eichmann K, Modolell M. Alternative metabolic states in murine macrophages reflected by the nitric oxide synthase/arginase balance: competitive regulation by CD4+ T cells correlates with Th1/Th2 phenotype. Journal of immunology (Baltimore, Md : 1950). 1998;160(11):5347-54.
51. Elgert KD, Alleva DG, Mullins DW. Tumor-induced immune dysfunction: the macrophage connection. Journal of leukocyte biology. 1998;64(3):275-90.
52. Solinas G, Germano G, Mantovani A, Allavena P. Tumor-associated macrophages (TAM) as major players of the cancer-related inflammation. Journal of leukocyte biology. 2009;86(5):1065-73.
53. Wynn TA, Barron L, Thompson RW, Madala SK, Wilson MS, Cheever AW, et al. Quantitative assessment of macrophage functions in repair and fibrosis. Current protocols in immunology / edited by John E Coligan [et al]. 2011;Chapter 14:Unit14 22.
54. Wynn TA. Fibrotic disease and the T(H)1/T(H)2 paradigm. Nat Rev Immunol. 2004;4(8):583-94.
55. Mantovani A, Sica A, Locati M. Macrophage polarization comes of age. Immunity. 2005;23(4):344-6.
56. Verreck FA, de Boer T, Langenberg DM, Hoeve MA, Kramer M, Vaisberg E, et al. Human IL-23-producing type 1 macrophages promote but IL-10-producing type 2 macrophages subvert immunity to (myco)bacteria. Proceedings of the National Academy of Sciences of the United States of America. 2004;101(13):4560-5.
57. Mosser DM, Edwards JP. Exploring the full spectrum of macrophage activation. Nat Rev Immunol. 2008;8(12):958-69.
58. Mantovani A, Schioppa T, Biswas SK, Marchesi F, Allavena P, Sica A. Tumor-associated macrophages and dendritic cells as prototypic type II polarized myeloid populations. Tumori. 2003;89(5):459-68.
59. Mantovani A, Allavena P, Sica A, Balkwill F. Cancer-related inflammation. Nature. 2008;454(7203):436-44.
60. Steding CE, Wu ST, Zhang Y, Jeng MH, Elzey BD, Kao C. The role of interleukin-12 on modulating myeloid-derived suppressor cells, increasing overall survival and reducing metastasis. Immunology. 2011;133(2):221-38.
61. Kuge S, Watanabe K, Makino K, Tokuda Y, Mitomi T, Kawamura N, et al. Interleukin-12 Augments the Generation of Autologous Tumor-reactive CD8+ Cytotoxic T Lymphocytes from Tumor-infiltrating Lymphocytes. Japanese Journal of Cancer Research. 1995;86(2):135-9.
62. Divino CM, Chen SH, Yang W, Thung S, Brower ST, Woo SL. Anti-tumor immunity induced by interleukin-12 gene therapy in a metastatic model of breast cancer is mediated by natural killer cells. Breast cancer research and treatment. 2000;60(2):129-34.

63. Menon C, Bauer TW, Kelley ST, Raz DJ, Bleier JI, Patel K, et al. Tumoricidal activity of high-dose tumor necrosis factor-alpha is mediated by macrophage-derived nitric oxide burst and permanent blood flow shutdown. International journal of cancer Journal international du cancer. 2008;123(2):464-75.
64. Sinha P, Clements VK, Ostrand-Rosenberg S. Reduction of myeloid-derived suppressor cells and induction of M1 macrophages facilitate the rejection of established metastatic disease. Journal of immunology (Baltimore, Md : 1950). 2005;174(2):636-45.
65. Arias-Salvatierra D, Silbergeld EK, Acosta-Saavedra LC, Calderon-Aranda ES. Role of nitric oxide produced by iNOS through NF-κB pathway in migration of cerebellar granule neurons induced by Lipopolysaccharide. Cellular Signalling. 2011;23(2):425-35.
66. Gordon S. Alternative activation of macrophages. Nat Rev Immunol. 2003;3(1):23-35.
67. Rodriguez PC, Quiceno DG, Zabaleta J, Ortiz B, Zea AH, Piazuelo MB, et al. Arginase I production in the tumor microenvironment by mature myeloid cells inhibits T-cell receptor expression and antigen-specific T-cell responses. Cancer research. 2004;64(16):5839-49.
68. Traves PG, Luque A, Hortelano S. Macrophages, inflammation, and tumor suppressors: ARF, a new player in the game. Mediators Inflamm. 2012;2012:568783.
69. Coussens LM, Werb Z. Inflammation and cancer. Nature. 2002;420(6917):860-7.
70. Biswas SK, Sica A, Lewis CE. Plasticity of macrophage function during tumor progression: regulation by distinct molecular mechanisms. Journal of immunology (Baltimore, Md : 1950). 2008;180(4):2011-7.
71. Qian BZ, Pollard JW. Macrophage diversity enhances tumor progression and metastasis. Cell. 2010;141(1):39-51.
72. Liguori M, Solinas G, Germano G, Mantovani A, Allavena P. Tumor-associated macrophages as incessant builders and destroyers of the cancer stroma. Cancers. 2011;3(4):3740-61.
73. Hao NB, Lu MH, Fan YH, Cao YL, Zhang ZR, Yang SM. Macrophages in tumor microenvironments and the progression of tumors. Clinical & developmental immunology. 2012;2012:948098.
74. Puig-Kroger A, Sierra-Filardi E, Dominguez-Soto A, Samaniego R, Corcuera MT, Gomez-Aguado F, et al. Folate receptor beta is expressed by tumor-associated macrophages and constitutes a marker for M2 anti-inflammatory/regulatory macrophages. Cancer research. 2009;69(24):9395-403.
75. Chanmee T, Ontong P, Konno K, Itano N. Tumor-associated macrophages as major players in the tumor microenvironment. Cancers. 2014;6(3):1670-90.
76. Pollard JW. Tumour-educated macrophages promote tumour progression and metastasis. Nat Rev Cancer. 2004;4(1):71-8.
77. Elisa Gomez Perdiguero FG. Identifying the infiltrators. Science (New York, NY). 2014;344 (6186):801-2.
78. Guruvayoorappan C. Tumor versus tumor-associated macrophages: how hot is the link? Integrative cancer therapies. 2008;7(2):90-5.
79. Jimenez B, Volpert OV. Mechanistic insights on the inhibition of tumor angiogenesis. Journal of molecular medicine (Berlin, Germany). 2001;78(12):663-72.
80. Uzzan B, Nicolas P, Cucherat M, Perret GY. Microvessel density as a prognostic factor in women with breast cancer: a systematic review of the literature and meta-analysis. Cancer research. 2004;64(9):2941-55.
81. Li W, Liang RR, Zhou C, Wu MY, Lian L, Yuan GF, et al. The association between expressions of Ras and CD68 in the angiogenesis of breast cancers. Cancer cell international. 2015;15(1):17.
82. Folkman J. Tumor angiogenesis: therapeutic implications. The New England journal of medicine. 1971;285(21):1182-6.
83. Bottini A, Berruti A, Bersiga A, Brizzi MP, Allevi G, Bolsi G, et al. Changes in microvessel density as assessed by CD34 antibodies after primary chemotherapy in human breast cancer. Clinical cancer research : an official journal of the American Association for Cancer Research. 2002;8(6):1816-21.
84. Locopo N, Fanelli M, Gasparini G. Clinical significance of angiogenic factors in breast cancer. Breast cancer research and treatment. 1998;52(1-3):159-73.

85. Wu Y, Zhou BP. Inflammation: a driving force speeds cancer metastasis. Cell cycle (Georgetown, Tex). 2009;8(20):3267-73.
86. Mantovani A, Marchesi F, Porta C, Sica A, Allavena P. Inflammation and cancer: breast cancer as a prototype. Breast (Edinburgh, Scotland). 2007;16 Suppl 2:S27-33.
87. Ribatti D, Nico B, Crivellato E. The role of pericytes in angiogenesis. The International journal of developmental biology. 2011;55(3):261-8.
88. Levine B, Kroemer G. Autophagy in the pathogenesis of disease. Cell. 2008;132(1):27-42.
89. Mizushima N. Autophagy: process and function. Genes & development. 2007;21(22):2861-73.
90. Martinez-Outschoorn UE, Balliet RM, Rivadeneira DB, Chiavarina B, Pavlides S, Wang C, et al. Oxidative stress in cancer associated fibroblasts drives tumor-stroma co-evolution: A new paradigm for understanding tumor metabolism, the field effect and genomic instability in cancer cells. Cell cycle (Georgetown, Tex). 2010;9(16):3256-76.
91. Martinez-Outschoorn UE, Whitaker-Menezes D, Pavlides S, Chiavarina B, Bonuccelli G, Casey T, et al. The autophagic tumor stroma model of cancer or "battery-operated tumor growth": A simple solution to the autophagy paradox. Cell cycle (Georgetown, Tex). 2010;9(21):4297-306.
92. Chen P, Cescon M, Bonaldo P. Autophagy-mediated regulation of macrophages and its applications for cancer. Autophagy. 2014;10(2):192-200.
93. Coussens LM, Pollard JW. Leukocytes in mammary development and cancer. Cold Spring Harbor perspectives in biology. 2011;3(3).
94. Mukhtar RA, Nseyo O, Campbell MJ, Esserman LJ. Tumor-associated macrophages in breast cancer as potential biomarkers for new treatments and diagnostics. Expert review of molecular diagnostics. 2011;11(1):91-100.
95. DeNardo DG, Brennan DJ, Rexhepaj E, Ruffell B, Shiao SL, Madden SF, et al. Leukocyte complexity predicts breast cancer survival and functionally regulates response to chemotherapy. Cancer discovery. 2011;1(1):54-67.
96. Aharinejad S, Paulus P, Sioud M, Hofmann M, Zins K, Schafer R, et al. Colony-stimulating factor-1 blockade by antisense oligonucleotides and small interfering RNAs suppresses growth of human mammary tumor xenografts in mice. Cancer research. 2004;64(15):5378-84.
97. Lin EY, Nguyen AV, Russell RG, Pollard JW. Colony-stimulating factor 1 promotes progression of mammary tumors to malignancy. The Journal of experimental medicine. 2001;193(6):727-40.
98. Chen J, Yao Y, Gong C, Yu F, Su S, Chen J, et al. CCL18 from Tumor-Associated Macrophages Promotes Breast Cancer Metastasis via PITPNM3. Cancer Cell. 2011;19(4):541-55.
99. Lewis CE, Leek R, Harris A, McGee JO. Cytokine regulation of angiogenesis in breast cancer: the role of tumor-associated macrophages. Journal of leukocyte biology. 1995;57(5):747-51.
100. Lin E, Gouon-Evans V, Nguyen A, Pollard J. The Macrophage Growth Factor CSF-1 in Mammary Gland Development and Tumor Progression. J Mammary Gland Biol Neoplasia. 2002;7(2):147-62.
101. Vaupel P, Kelleher DK, Hockel M. Oxygen status of malignant tumors: pathogenesis of hypoxia and significance for tumor therapy. Seminars in oncology. 2001;28(2 Suppl 8):29-35.
102. Murdoch C, Giannoudis A, Lewis CE. Mechanisms regulating the recruitment of macrophages into hypoxic areas of tumors and other ischemic tissues. Blood. 2004;104(8):2224-34.
103. Turner L, Scotton C, Negus R, Balkwill F. Hypoxia inhibits macrophage migration. European journal of immunology. 1999;29(7):2280-7.
104. Leek RD, Lewis CE, Whitehouse R, Greenall M, Clarke J, Harris AL. Association of macrophage infiltration with angiogenesis and prognosis in invasive breast carcinoma. Cancer research. 1996;56(20):4625-9.
105. Lee YT. Breast carcinoma: pattern of metastasis at autopsy. Journal of surgical oncology. 1983;23(3):175-80.
106. Condeelis J, Pollard JW. Macrophages: obligate partners for tumor cell migration, invasion, and metastasis. Cell. 2006;124(2):263-6.
107. Bonapace L, Coissieux MM, Wyckoff J, Mertz KD, Varga Z, Junt T, et al. Cessation of CCL2 inhibition accelerates breast cancer metastasis by promoting angiogenesis. Nature. 2014;515(7525):130-3.

108. Lewis JS, Landers RJ, Underwood JC, Harris AL, Lewis CE. Expression of vascular endothelial growth factor by macrophages is up-regulated in poorly vascularized areas of breast carcinomas. The Journal of pathology. 2000;192(2):150-8.
109. Jemal A, Bray F, Center MM, Ferlay J, Ward E, Forman D. Global cancer statistics. CA: a cancer journal for clinicians. 2011;61(2):69-90.
110. Wang Y, Zhou BP. Epithelial-mesenchymal Transition---A Hallmark of Breast Cancer Metastasis. Cancer hallmarks. 2013;1(1):38-49.
111. Fantozzi A, Christofori G. Mouse models of breast cancer metastasis. Breast Cancer Res. 2006;8(4):212.
112. Junttila MR, de Sauvage FJ. Influence of tumour micro-environment heterogeneity on therapeutic response. Nature. 2013;501(7467):346-54.
113. Khanna C, Hunter K. Modeling metastasis in vivo. Carcinogenesis. 2005;26(3):513-23.
114. Talmadge JE, Singh RK, Fidler IJ, Raz A. Murine models to evaluate novel and conventional therapeutic strategies for cancer. The American journal of pathology. 2007;170(3):793-804.
115. Huss WJ, Maddison LA, Greenberg NM. Autochthonous mouse models for prostate cancer: past, present and future. Semin Cancer Biol. 2001;11(3):245-60.
116. Dexter DL, Kowalski HM, Blazar BA, Fligiel Z, Vogel R, Heppner GH. Heterogeneity of tumor cells from a single mouse mammary tumor. Cancer research. 1978;38(10):3174-81.
117. Miller FR, Miller BE, Heppner GH. Characterization of metastatic heterogeneity among subpopulations of a single mouse mammary tumor: heterogeneity in phenotypic stability. Invasion & metastasis. 1983;3(1):22-31.
118. Aslakson CJ, Miller FR. Selective events in the metastatic process defined by analysis of the sequential dissemination of subpopulations of a mouse mammary tumor. Cancer research. 1992;52(6):1399-405.
119. Lou Y, Preobrazhenska O, auf dem Keller U, Sutcliffe M, Barclay L, McDonald PC, et al. Epithelial-mesenchymal transition (EMT) is not sufficient for spontaneous murine breast cancer metastasis. Developmental dynamics : an official publication of the American Association of Anatomists. 2008;237(10):2755-68.
120. Issa A, Gill JW, Heideman MR, Sahin O, Wiemann S, Dey JH, et al. Combinatorial targeting of FGF and ErbB receptors blocks growth and metastatic spread of breast cancer models. Breast Cancer Res. 2013;15(1):R8.
121. LSM 510 and LSM 510 META Laser Scanning Microscopes Operating Manual Release 3.2. Germany: Carl Zeiss Advanced Imaging Microscopy; 2002.
122. QIAGEN. Critical Factors for Successful Real-Time PCR 2009. Available from: http://www.ff.ul.pt/~mjgama/Critical_Factors_for_Successful_Real-Time_PCR%5B1%5D.pdf.
123. QIAGEN. RNAprotect® Cell Reagent Handbook 2010. Available from: https://www.qiagen.com/no/resources/resourcedetail?id=bea04757-b25e-4eb1-86b4-3ef1cb4f94b0&lang=en.
124. SCIENTIFIC T. NanoDrop 1000 Spectrophotometer V3.7 User's Manual 2008. Available from: http://www.nanodrop.com/library/nd-1000-v3.7-users-manual-8.5x11.pdf.
125. QIAGEN. QuantiTect® Reverse Transcription Handbook 2009. Available from: https://www.qiagen.com/no/resources/resourcedetail?id=f0de5533-3dd1-4835-8820-1f5c088dd800&lang=en.
126. technologies L. PRODUCT BULLETIN TaqMan®SNP Genotyping Assays.6.
127. Custom TaqMan®Assays For New SNP Genotyping and Gene Expression Assays Design and Ordering Guide. 2010.
128. QIAGEN. QIAGEN Genomic DNA Handbook 2001. Available from: https://www.qiagen.com/no/resources/resourcedetail?id=402bb209-4104-4956-a005-6226ff0b67d5&lang=en.
129. Molecular Therapeutics for Cancer IM. BreastMark. Available from: http://glados.ucd.ie/BreastMark/.

130. Parker JS, Mullins M, Cheang MC, Leung S, Voduc D, Vickery T, et al. Supervised risk predictor of breast cancer based on intrinsic subtypes. J Clin Oncol. 2009;27(8):1160-7.
131. Chen F, Guo N, Cao G, Zhou J, Yuan Z. Molecular analysis of curcumin-induced polarization of murine RAW264.7 macrophages. J Cardiovasc Pharmacol. 2014;63(6):544-52.
132. Movahedi K, Laoui D, Gysemans C, Baeten M, Stange G, Van den Bossche J, et al. Different tumor microenvironments contain functionally distinct subsets of macrophages derived from Ly6C(high) monocytes. Cancer research. 2010;70(14):5728-39.
133. Place AE, Jin Huh S, Polyak K. The microenvironment in breast cancer progression: biology and implications for treatment. Breast Cancer Res. 2011;13(6):227.
134. Biswas SK, Gangi L, Paul S, Schioppa T, Saccani A, Sironi M, et al. A distinct and unique transcriptional program expressed by tumor-associated macrophages (defective NF-kappaB and enhanced IRF-3/STAT1 activation). Blood. 2006;107(5):2112-22.
135. Kunz-Schughart LA, Weber A, Rehli M, Gottfried E, Brockhoff G, Krause SW, et al. [The "classical" macrophage marker CD68 is strongly expressed in primary human fibroblasts]. Verh Dtsch Ges Pathol. 2003;87:215-23.
136. Mouawad R, Spano JP, Khayat D. Lymphocyte infiltration in breast cancer: a key prognostic factor that should not be ignored. J Clin Oncol. 2011;29(15):1935-6.
137. Zhang Y, Cheng S, Zhang M, Zhen L, Pang D, Zhang Q, et al. High-infiltration of tumor-associated macrophages predicts unfavorable clinical outcome for node-negative breast cancer. PloS one. 2013;8(9):e76147.
138. O'Sullivan C, Lewis CE. Tumour-associated leucocytes: friends or foes in breast carcinoma. The Journal of pathology. 1994;172(3):229-35.
139. Biosystems A. TaqMan®SNP Genotyping Assays Protocol. 2010:60.
140. Casazza A, Laoui D, Wenes M, Rizzolio S, Bassani N, Mambretti M, et al. Impeding Macrophage Entry into Hypoxic Tumor Areas by Sema3A/Nrp1 Signaling Blockade Inhibits Angiogenesis and Restores Antitumor Immunity. Cancer Cell. 2013;24(6):695-709.
141. Wyckoff JB, Wang Y, Lin EY, Li JF, Goswami S, Stanley ER, et al. Direct visualization of macrophage-assisted tumor cell intravasation in mammary tumors. Cancer research. 2007;67(6):2649-56.
142. Laoui D, Movahedi K, Van Overmeire E, Van den Bossche J, Schouppe E, Mommer C, et al. Tumor-associated macrophages in breast cancer: distinct subsets, distinct functions. The International journal of developmental biology. 2011;55(7-9):861-7.
143. Lloyd CM, Phillips AR, Cooper GJ, Dunbar PR. Three-colour fluorescence immunohistochemistry reveals the diversity of cells staining for macrophage markers in murine spleen and liver. J Immunol Methods. 2008;334(1-2):70-81.
144. Sica A, Mantovani A. Macrophage plasticity and polarization: in vivo veritas. The Journal of clinical investigation. 2012;122(3):787-95.
145. Gao S, Wang L, Liu W, Wu Y, Yuan Z. The synergistic effect of homocysteine and lipopolysaccharide on the differentiation and conversion of raw264.7 macrophages. J Inflamm (Lond). 2014;11:13.
146. Goswami S, Sahai E, Wyckoff JB, Cammer M, Cox D, Pixley FJ, et al. Macrophages promote the invasion of breast carcinoma cells via a colony-stimulating factor-1/epidermal growth factor paracrine loop. Cancer research. 2005;65(12):5278-83.
147. Chamberlain LM, Godek ML, Gonzalez-Juarrero M, Grainger DW. Phenotypic non-equivalence of murine (monocyte-) macrophage cells in biomaterial and inflammatory models. J Biomed Mater Res A. 2009;88(4):858-71.
148. Edin S, Wikberg ML, Dahlin AM, Rutegard J, Oberg A, Oldenborg PA, et al. The distribution of macrophages with a M1 or M2 phenotype in relation to prognosis and the molecular characteristics of colorectal cancer. PloS one. 2012;7(10):e47045.
149. Erin N, Kale S, Tanriover G, Koksoy S, Duymus O, Korcum AF. Differential characteristics of heart, liver, and brain metastatic subsets of murine breast carcinoma. Breast cancer research and treatment. 2013;139(3):677-89.

150. Liu R, Wang X, Chen GY, Dalerba P, Gurney A, Hoey T, et al. The prognostic role of a gene signature from tumorigenic breast-cancer cells. The New England journal of medicine. 2007;356(3):217-26.
151. Tacke F, Alvarez D, Kaplan TJ, Jakubzick C, Spanbroek R, Llodra J, et al. Monocyte subsets differentially employ CCR2, CCR5, and CX3CR1 to accumulate within atherosclerotic plaques. The Journal of clinical investigation. 2007;117(1):185-94.
152. Lindquist RL, Shakhar G, Dudziak D, Wardemann H, Eisenreich T, Dustin ML, et al. Visualizing dendritic cell networks in vivo. Nat Immunol. 2004;5(12):1243-50.
153. Visvader JE. Keeping abreast of the mammary epithelial hierarchy and breast tumorigenesis. Genes & development. 2009;23(22):2563-77.

Appendix

I Cell types and markers that can be investigated in breast tumor

Cell type	Markers (Mouse)	Marker (Human)	Reference
Myeloid lineage			
Macrophages general marker	Adgre1	F4/80	(21, 39, 134)
	Cd68	CD68	(47, 134)
M1 Macrophages	Cd40, Fcgr1	CD40, CD64	(41)
	Cd74	MHCII	(132)
	Nos2	NOS2	(134, 148)
M2 Macrophages	Arg1	ARG1	(66, 134)
	Cd163	CD163	(41, 148)
Fibroblast	Vim	VIM	(19)
Epithelial	Cd44, Cd24	CD44, CD24	(149, 150)
Monocytes	Csf1r	CSF1R	(39)
Dendritic cell	Itgax	CD11c	(21, 151, 152)
Neutrophil	Itgam	CD11b	(39)
Tie-2-expresing monocytes(TEM)	Cd14, Itgam	CD14, CD11b	(19)
Myeloid derived suppressor cells (MDSCs)	Itgam	Cd11b	(21, 32)
Vessel endothelial	Cd34	CD34	(81)
Mast cell	Cd203c	CD203c	(21)
Lymphoid lineage			
B cell	Cd19	CD19	(21)
T cell	Itga6	ITGA6 (CD49f)	(153)
NK cell	Ncr1	NCR1 (CD335)	(21)

II Chromosome 1 sequence (base of primer and probe design)

Name: 66-67chr1
TCATGCTTGAGCCGCCGATGCTGCTGAAGGCACCGGCTTTGTTTGCAGGTAAAGCCACAGTCCCCAC
ACTGCAGGAGGGGCCGGGGGCCAGAGGCTGGGGATGCAGTGGGATGCCTCCGTTTTTGATGGAGC
CTCAGGNNNNNNNNNNNNGGAGCAGTGAATGGGCAGAGACCACAGTGCAGATCTCCAGACTTAA
GGGGGCAGCCCTGGGTCTGGTGAGTCCTCAGGGTCCTTTCCTGCTGACAGCTAAAGGGACATGTGG
GGCAGGAGAAGAGGGCACCCTTTTGCTTCTGAACCACAGCTGTGTCCCCATCACTAGGACTGGACTC
TGTACTTCCAGTATTCAGGAGGGTAGAGTCCCCATTGTTAAGAGGAAGCACAACTGCATGGGTCTGG
GGGC[G/A]CCCACGCTTTCTTTTCTGGCCACGCCCCCCTCTACAGCCTTCAGTCACATGAGAGGTAAT
AGAAGAAAGCCGAGAACAAAGGAATGTACACGAGCTGCAGTGAAACTTGCCTTGCTCAAAGTGGAA
CTTCTCAGAGGTCCCTGTGGGTAAGGAGTTTTCTGGTGGAGAGGTTGGGAAGTCAGAGGGTGTGGG
AAGAGGTTCCTCTACTCCTGGCCCCCCAGGGAGGTCAGAAGGAGCATCTTTTGGAAGCAAGAGCTCT
ACCTTTGATGGTAAAGGTGGGGGCTTCCTACTTTCAGCATCCTGTGAGGCTTGGTTATCTGGGAGCT
GAGGATGTAGAGTGGGAGAGACAGGTTTGGGCAAAGCCTTGTTCTTTTTGAGAAGAACAGGGCATT
TCTTCATC